William & Mary
CHARTERED 1693

W&M ScholarWorks

Reports

1-1-1999

Modeling Coastal Hydrodynamics and Water Qualityof Kyunggi Bay Korea:Application of VIMS HEM-3D Model

Jian Shen
Virginia Institute of Marine Science

Chang-Shik Kim
Virginia Institute of Marine Science

Albert Y. Kuo
Virginia Institute of Marine Science

Follow this and additional works at: https://scholarworks.wm.edu/reports

 Part of the Marine Biology Commons

Recommended Citation

Shen, J., Kim, C., & Kuo, A. Y. (1999) Modeling Coastal Hydrodynamics and Water Qualityof Kyunggi Bay Korea:Application of VIMS HEM-3D Model. Special Reports in Applied Marine Science and Ocean Engineering (SRAMSOE) No. 350. Virginia Institute of Marine Science, College of William and Mary. http://dx.doi.org/doi:10.21220/m2-1vq1-k911

This Report is brought to you for free and open access by W&M ScholarWorks. It has been accepted for inclusion in Reports by an authorized administrator of W&M ScholarWorks. For more information, please contact scholarworks@wm.edu.

Modeling Coastal Hydrodynamics and Water Quality of Kyunggi Bay Korea: Application of VIMS HEM-3D Model

by
Jian Shen, Chang-Shik Kim, Sung-Chan Kim and Albert Y. Kuo

A Report to the
Korea Ocean Research and Development Institute
Ansan, Korea

Special Report No. 350
In Applied Marine Science and Ocean Engineering

School of Marine Science / Virginia Institute of Marine Science
The College of William and Mary in Virginia
Gloucester Point, Virginia 23062

VIMS
GC
1
S67
no.350

January 1999

VIMS
GC
1
S67
no. 350

MODELING COASTAL HYDRODYNAMICS AND WATER QUALITY OF KYUNGGI BAY, KOREA: APPLICATION OF VIMS HEM-3D MODEL

by

Jian Shen, Chang-Shik Kim, Sung-Chan Kim and Albert. Y. Kuo

LIBRARY
VIRGINIA INSTITUTE
of
MARINE SCIENCE

A Report to the
Korea Ocean Research and Development Institute
Ansan, Korea

Special Report No. 350
In Applied Marine Science and Ocean Engineering

School of Marine Science/Virginia Institute of Marine Science
The College of William and Mary in Virginia
Gloucester Point, VA 23062

January 1999

Table of Contents

List of Figures

ACKNOWLEDGEMENTS

The authors are indebted to Dr. John M. Hamrick, developer of the Environmental Fluid Dynamics code (EFDC) which provides the hydrodynamic base code of the VIMS three dimensional Hydrodynamic-Eutrophication Model (HEM-3D). We also owe thanks to Dr. Kyeong Park who first implemented water quality module to the HEM-3D model. This application of VIMS HEM-3D model to Kyunggi Bay, Korea was performed under a contract 'Joint Development of Program for Real-Time Ocean and Benthic Environment Modeling System' between Virginia Institute of Marine Science and Korea Ocean Research and Development Institute (KORDI). The financial support from KORDI is hereby acknowledged.

I. Introduction

VIMS has developed the HEM-3D model—a general purpose three-dimensional Hydrodynamic-Eutrophication Model. It is uniquely suited to estuaries and coastal seas. The model has been applied to a wide range of environmental studies in the Chesapeake Bay and its tributaries (e.g., Shen et al., 1997; Hamrick et. al., 1995; Hamrick, 1992a, 1992b) and other systems (e.g., Kim et al., 1997; Moustafa and Hamrick, 1994).

The model consists of two parts—the hydrodynamic part and water quality part. The Environmental Fluid Dynamics Code (EFDC; Hamrick, 1992a, 1996) constitutes the hydrodynamic portion of the HEM-3D. The EFDC model developed by Hamrick (1992a) resembles the widely used Blumberg-Mellor model (Blumberg and Mellor, 1987) in both the physics and the computational scheme utilized. The model solves the three-dimensional, vertical hydrostatic, free surface equations of motion and responds to surface wind stress, heat and salinity fluxes, freshwater discharge and specification of tidal forcing. Mellor and Yamada level 2.5 turbulence closure scheme was implemented in the model (Mellor and Yamada 1982; Gulperin et. al 1988). The model uses stretched (or sigma) vertical coordinate and Cartesian or curvilinear, orthogonal horizontal coordinates. The model uses a second-order accurate, three-time-level finite difference scheme with an internal-external mode splitting procedure to separate the internal shear or baroclinic mode from the external free surface gravity wave. The external mode solution uses a semi-implicit scheme to allow large time steps that are constrained only by the stability criteria of the explicit central difference or upwind advection scheme used for the nonlinear accelerations. The model simulates density and topographically-induced

circulation as well as tidal and wind-driven flows, and spatial and temporal distributions of salinity, temperature and suspended sediment concentration.

Both water quality model with 21 state variables and a sediment process model with 27 state variables (Cerco and Cole, 1993) have been developed and linked to EFDC to form the HEM-3D (Park et al. 1995). The model simulates the spatial and temporal distributions of water quality parameters including dissolved oxygen, suspended algae, various components of carbon, nitrogen, phosphorus and silica cycles, and fecal coliform bacteria. The sediment process model, upon receiving the particulate organic matter deposited from the overlying water column, simulates their diagenesis and resulting fluxes of inorganic substances and sediment oxygen demand back to the water column. Other transport models are currently being coupled with the hydrodynamic model that predict the movement and distribution of a scalar quantity (e.g., mass concentration of marine larvae, toxins or dredged material). These scalars may be modeled as either conservative or non-conservative quantities that are either coupled or de-coupled with the fluid (e.g., sediment particle with finite settling velocity). In the HEM-3D, scalar quantities are usually introduced into the model domain as a point source and then followed over a time scale of hours and days.

The HEM-3D model code is written in standard FORTRAN 77 and is portable to variable computing platforms. It is computationally efficient due to the programmer's avoidance of logical operators, and it economizes on required storage by storing only active water cell variables in memory. This code was written to be highly vectorizable, anticipating upcoming developments in parallel processing. Due to a well-designed user interface, the internal source code remains the same from application to application. The

HEM-3D model can be quickly converted to a 2D model either horizontally or vertically for preliminary testing. The model's most unique features include the mass conservative scheme for drying and wetting in shallow areas. It also incorporates vegetation resistance formulations (Hamrick, 1994). The most valuable feature is the model's ability to couple with both water quality and sediment transport models.

This report will attempt to provide a detailed documentation for the HEM-3D model application to the Kyunggi Bay and the adjacent Yellow Sea. The main objective is to demonstrate the applicability of the HEM-3D to Kyunggi Bay which is characterized as shallow macrotidal environment with complicated coastal geometry. One of the critical point to apply the HEM-3D model is the success of wet-and-dry scheme. First, hydrodynamic portion of the HEM-3D model was tested. Then, the applicability of water quality model was tested by investigating conservative transport of substance.

II. Model Setup

II.1. Structure of input files

Model configuration and environmental data for a particular application are provided in the following sequence of input files (in alphabetical order):

File Name	Type of Input Data
aser.inp	Atmospheric forcing time series file.
cell.inp	Horizontal cell type identifier file.
celllt.inp	Horizontal cell type identifier file for saving mean mass transport.
depth.inp	File specifying depth, bottom elevation, and bottom roughness for Cartesian grids only.
dser.inp	Dye concentration time series file.
dxdy.inp	File specifying horizontal grid spacing or metrics, depth, bottom levation, bottom roughness and vegetation classes for either Cartesian or curvilinear-orthogonal horizontal grids.
dye.inp	File with initial dye distribution for cold start simulations.
efdc.inp	Master input file.
fldang.inp	File specifying the CCW angle to the flood axis of the local M2 tidal ellipses.
gcellmap.inp	File specifying a Cartesian grid overlay for a curvilinear-orthogonal grid.
gwater.inp	File specifying the characteristic of a simple soil moisture model.
lxly.inp	File specifying horizontal cell center coordinates and cell orientations for either Cartesian or curvilinear-orthogonal grids.
mappgns.inp	Specifies configuration of the model grid to represent a periodic region in the north-south or computational y direction.
mask.inp	File specifying thin barriers to block flow across specified cell faces.
modchan.inp	Subgrid scale channel model specification file.

moddxdy.inp	File specifying modification to cell sizes. (used primarily for calibration adjustment of subgrid scale channel widths)
pser.inp	Open boundary water surface elevation time series file.
qctl.inp	Hydraulic control structure characterization file.
qser.inp	Volumetric source-sink time series file.
restart.inp	File for restarting a simulation.
restran.inp	File with arbitrary time interval averaged transport fields used to drive mass transport only simulations.
salt.inp	File with initial salinity distribution for cold start, salinity stratified flow simulations.
sdser.inp	Suspended sediment concentration time series file.
show.inp	File controlling screen print of conditions in a specified cell during simulation runs.
sser.inp	Salinity time series file.
sfser.inp	Shellfish release time series file.
sfbser.inp	Shellfish behavior time series file.
tser.inp	Temperature time series file.
vege.inp	Vegetation resistance characterization file.
wave.inp	Specifies a high frequency surface gravity wave field require to activate the wave-current boundary layer model and/or wave induced current model.

The above listed input files can be classified in five groups as follows:

- Horizontal grid specification files—cell.inp, celllt.inp, depth.inp, dxdy.inp, gcellmap.inp, lxly.inp, mappgns.inp,mask.inp
- General data and run control files—efdc.inp, show.inp
- Initialization and restart files—salt.inp, dye.inp, restart.inp, restran.inp

- Physical process specification files—gwater.inp, modchan.inp, moddxdy.inp, qctl.inp, vege.inp, wave.inp

- Time series forcing and boundary condition files—aser.inp, dser.inp, pser.inp, qser.inp, sdser.inp, sfser.inp, sfbser.inp, sser.inp, sser.inp

II.2. Grid

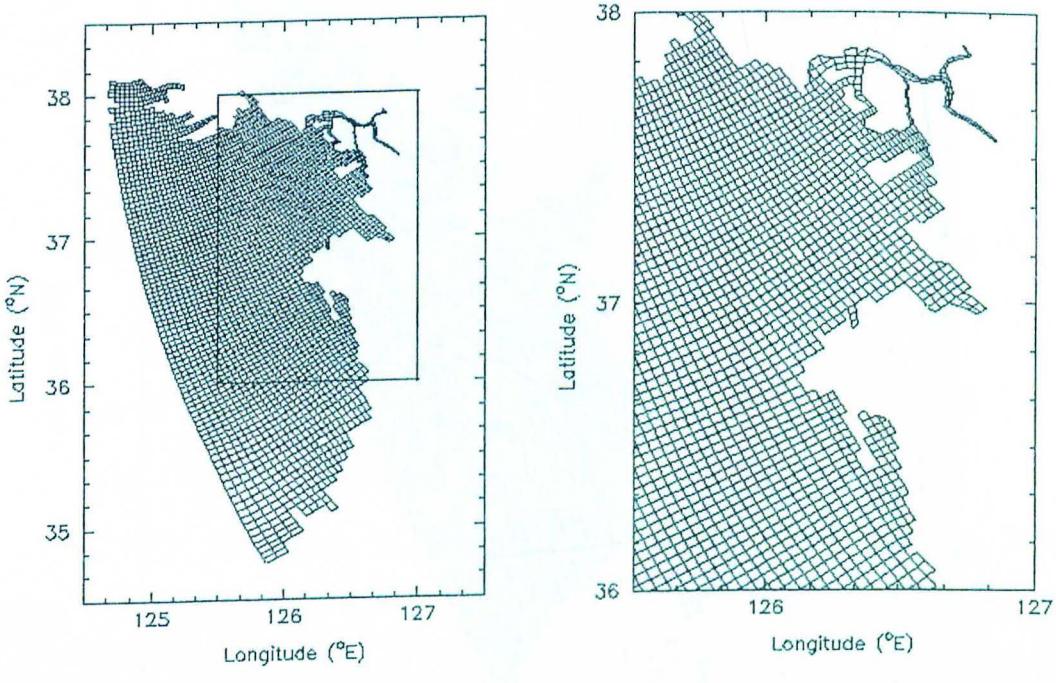

Figure 1. HEM-3D model grid for Kyunggi Bay, Korea

Appendix A shows the grid information input file "CELL.INP" in which 78 by 96 horizontal grid cells cover the model domain. Total number of active water cells is 3122. The generated curvilinear grid has a higher resolution near Inchon (~ 1 km) and lower

resolution at open boundary and south (~ 3 km) (Figure 1). Han River was included as a major connecting estuary. Figure 2 shows depths of grid cells.

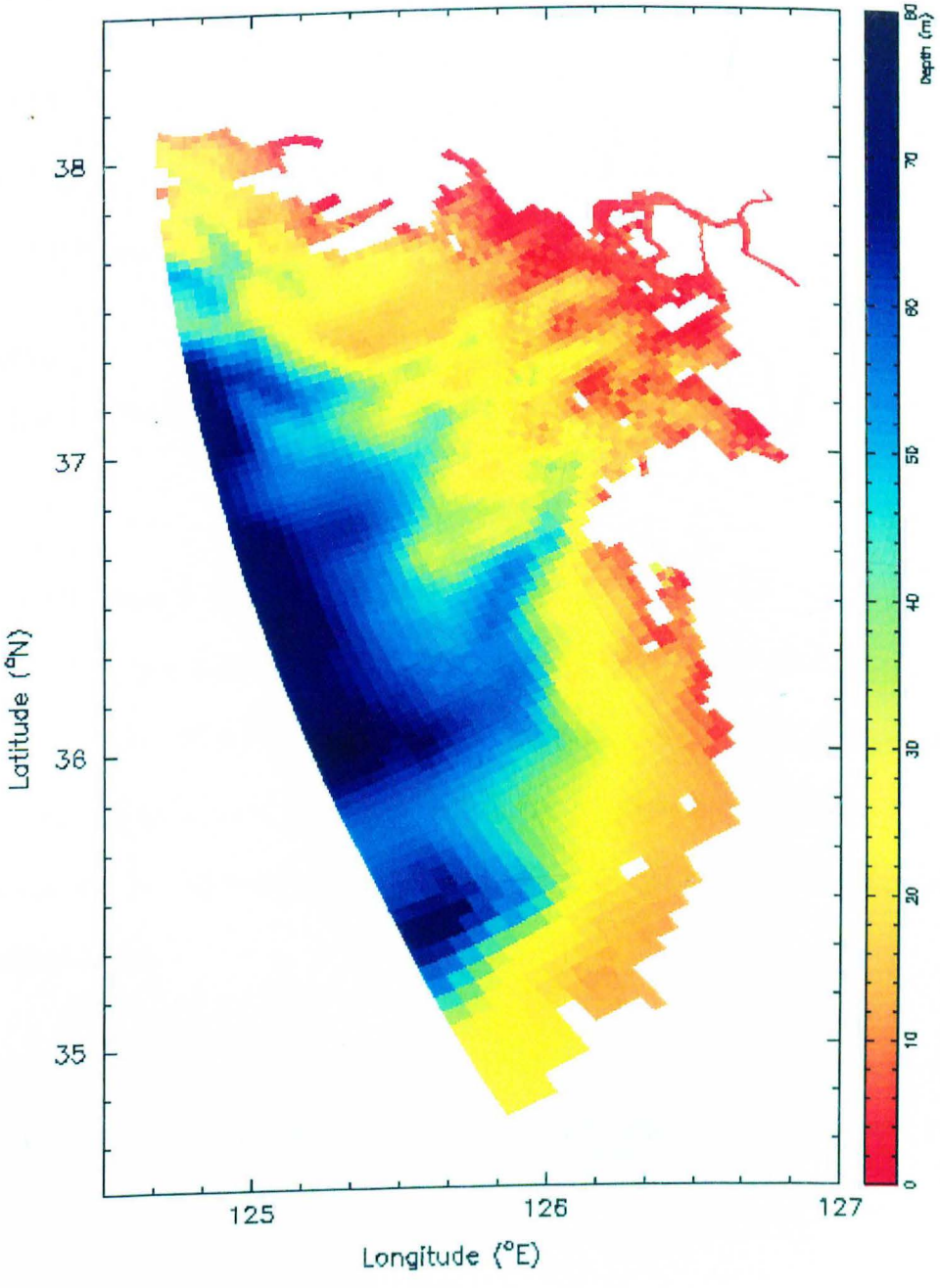

Figure 2. HEM-3D grid depth for Kyunggi Bay

II.3. Model run

The following discusses the detail of model setup given by "EFDC.INP". Parameters are described by Hamrick (1996) in detail.

Card Image 1

```
C1   TITLE FOR RUN
KYUNGGI BAY HEM-3D SIMULATION FOR KORDI. 5-11-98.
```

Card Image 1 specifies the title of the run setup.

Card Image 2

```
C2 ISRESTI ISRESTO ISRESTR ISPAR ISLOG ISDIVEX ISNEGH ISMMC ISBAL ISHP ISHOW
     1       4       0      0     2     0       0      0     0     0    0
```

Card Image 2, specifies the mode of model startup. IRESTI=1 states using initial conditions corresponding to the conditions at the end of a previous simulation, given by "RESTART.INP". ISRESTO=4 switch controls the frequency of outputting (every 4 days) restart information to the file "RESTART.OUT" (which is renamed "RESTART.INP" to launch a run). The switch ISLOG=2 activates the creation of a log file "EFDC.LOG"

Card Image 3

```
C3   RP   RSQM   ITERM IRVEC RPADJ RSQMADJ ITRMADJ ITERHPM IDRYCK ISDSOLV
    1.8 1.E-12  400  2      1.8   1.E-16   1000      1         10        0
```

Card Image 3 includes controls of the external or barotropic mode solution. The relaxation parameter of 1.8 should not be changed. The RSQM parameter is the residual

squared error in the external mode solution and taken as 1.E-12. The maximum iteration count in the external solution ITERM is set such that execution stops if the external solution does not converge in the maximum number of 400 iterations. The parameter IRVEC=2 states that the original successive over relaxation solver has been supplemented with two diagonally preconditioned conjugate gradient solver. IRVEC = 2, is required when drying and wetting is activated. IDRYCK=10 states wet-and-dry check every iteration.

Card Image 4

```
C4    ISLTMT   ISSSMMT ISLTMTS   ISIA   RPIA   RSQMIA    ITRMIA
       0        0        0        0     1.8    1.E-10    100
```

In this model, a transport only mode is not utilized.

Card Image 5

```
ISCDMA ISAHMF ISDISP ISWASP ISDRY ISQQ ISRLID ISVEG ISVEGL ISITB ISWAVE
    0      0      0      0     11     1     0      0      0      0      0
```

ISDRY=11 means that constant wetting depth specified by HWET (= 0.15 m) in Card 11 with nonlinear iterations specified by ITERHPM on Card 3 (= 1) without nonlinear iteration.

Card Image 6

```
ISTRAN ISTOPT ISCDCA ISADAC ISFCT ISPLIT ISADAH ISADAV ISCI ISCO
1      0      0      0      0     0      0      0      0    0     !tur 0
```

```
1       1       0       1       1       0       0       0       1       1       !sal 1
0       3       0       0       0       0       0       0       0       0       !tem 2
0       0       0       0       0       0       0       0       0       0       !dye 3
1       1       0       1       1       0       0       0       0       0       !sed 4
0       0       0       0       0       0       0       0       0       0       !snd 5
0       0       0       1       1       0       0       0       0       0       !tox 6
0       1       0       1       1       0       0       0       0       0       !sfl 7
1       0       1       0       0       0       0       0       0       0       !cwq 8
```

Turbulence, salinity, sediment, and water quality were activated. For salinity, initial salinity distribution was read from file "RESTART.INP" (ISCI=1) and final results were written to "RESTART.OUT" (ISCO=1) at the end of the run. Cohesive sediment was assumed for suspended sediment transport (ISOPT=1). Except for water quality (ISCDCA=1), upwind difference schemes and anti-numerical diffusion schemes were used.

Card Image 7

```
NTC   NTSPTC NLTC NTTC NTCPP NTSTBC NTCNB NTCVB NTSMMT NFLTMT   NDRYSTP
10    1200    0    0   960   8       0     1     960    1        4
```

Card Image 8

```
TCON    TBEGIN   TREF     CORIOLIS    ISCCA   ISCFL
3600    0.00     86400    8.77e-5     0       0
```

Card Images 7 and 8 provide time controls for the simulation with Card Image 7 providing integer parameters. 10 day simulation was done (NTC = 10). For one day cycle (TREF = 86400 seconds), total 1200 time steps (NTSPTC) were put in, giving 72 second time step. Minimum number of time steps a cell remains dry after initial drying (NDRYSTP) was set as 4. TBEGIN specifies the start time of the runs in units of seconds, minutes, hours, or days, with TCON being the multiplier factor which would

convert TBEGIN to seconds. The reference time period must always be specified in seconds. The HEM-3D model currently is based on an f plane formulation for the Coriolis accelerations, with the variable CORIOLIS being the value of f in 1/seconds units.

Card Image 9

```
KC IC JC   LC LVC ISCO NDM LDW ISMASK ISPGNS NSHMX NSBMX  WSMH    WSMB
6  78 96 3124 3122 1    1  3122 0     0      5     0      0.03125 0.5
```

Card Image 10

```
C10  LAYER NUMBER    DIMENSIONLESS LAYER THICKNESS
       1                 0.166
       2                 0.167
       3                 0.167
       4                 0.167
       5                 0.167
       6                 0.166
```

Card Image 11

```
DX DY  DXYCVT ZBRADJ ZBRCVRT HMIN HMADJ HCVRT HDRY HWET BELADJ BELCVRT|
1. 1.   1.    0.0002  0.0     0.22 0.0  1.0   0.10 0.15  0.0    1.0
```

Card images 9, 10 and 11 specify the spatial structure of the model grid. Vertically 6 layers (KC) were set in σ-coordinate (evenly spaced as 1/6 of total depth). Horizontally, IC (= 78) by JC (= 96) were set in the computational x and y directions. Total number of active cells were given by LVC (= 3122). ISCO=1 denotes curvilinear grid was used. For depth smoothing, 5 passes (NSHMAX) with weight (WSMH = 0.03125) was used. For salinity 0.5 was used for the weight (WSMB). The conversion factor DXYCVT can be used to convert the units of DX and DY in the "DXDY.INP" to the required internal unit of meters. The parameters ZBRADJ and ZBRCVRT are used

to adjust and convert the log law, *zo*, bottom roughness specified in the "DXDY.INP". The conversion equation is of the form is:

ZBR=ZBRADJ + ZBRCVRT*ZBR

The parameter HMIN is used to specify a minimum depth, over- riding input values. The parameters HADJ and HCVRT and BEADJ and BECVRT provide for adjustments and conversions to the initial depth and bottom elevation inputs in the same format as that for bottom roughness. The parameter HDRY specifies the water depth at which a cell becomes dry, while HWET specifies the depth at which the cell become wet.

Card Image 12

```
C12  AHO    AHD      AVO       ABO       AVBCON   ISFAVB
     0.0    0.0      1.E-6     1.E-8     1.0      1
```

Card Image 13

```
C13  VKC    CTURB    CTE1    CTE2    CTE3    QQMIN    QQLMIN    DMLMIN
     0.4    16.0     1.8     1.33    0.53    1.E-8    1.E-16    1.E-6
```

Card images 12 and 13 provide information for horizontal and vertical momentum and mass diffusion throughturbulence closure parameter. A spatially constant horizontal diffusion is specified by a constant value AHO. A variable horizontal diffusion may be added to the constant value by specifying a non- zero value of AHD, which is the dimensionless constant in the Smagorinsky subgrid scale horizontal diffusion formulation (Smagorinsky, 1963). The background molecular kinematic viscosity and diffusivity are specified by AVO and ABO respectively. When AVBCON is set to 0, the turbulence

model is deactivated and the vertical viscosity and diffusivity are set to AVO and ABO respectively. Using this option and setting AVO and ABO to larger values representing turbulent flow readily allows model results to be compared with constant viscosity and diffusivity analytical solutions for vertical current structure. Setting the parameter ISFAVB to 1 activates a square root smoother for both the vertical turbulent viscosity and diffusivity of the form:

$$AVO(n+1)=SQRT(AVO(n+1)*AVO(n))$$

where n indicates the timestep. The smoother is particularly useful for flows having strong surface wind stress forcings.

Card Image 14

```
C14   MTIDE   ISLSHA   MLLSHA    NTCLSHA   ISLSTR    ISHTA
        1        1        8         2         0         0
```

Card Image 15

```
C15   SYMBOL     PERIOD
        'M2'     44714.16
```

Card Image 16

```
C16   ILLSHA    JLLSHA     LSHAP   LSHAB   LSHAUE   LSHAU    CLSL
        58         55         1       0        1       1     'Inchon'
        27         17         1       0        1       1     'Kunsan'
        27         41         1       0        1       1     'Auhung'
        30         28         1       0        1       1     'Wonsando'
        34         53         1       0        1       1     'Sungapdo'
         3         87         1       0        1       1     'Daechungdo'
        39         56         1       0        1       1     'Duckjuckdo'
        59         56         1       0        1       1     'Inchon 2'
```

Card Image 17

```
C17   NPBS  NPBW  NPBE  NPBN   NPFOR   NPSER   PDGINIT
        0     90    0     0      90      0       0.00
```

Card Image 18

C18	NPFOR	SYMBOL	AMPLITUDE		PHASE
	1	M2"	1.1409	2412.00	1.09
	2	M2"	1.1427	2563.20	1.09
	3	M2"	1.1439	2901.60	1.09
	4	M2"	1.1443	3232.80	1.09
	5	M2"	1.1465	3553.20	1.09
	6	M2"	1.1498	3934.80	1.09
	7	M2"	1.1522	4287.60	1.09
	8	M2"	1.1560	4658.40	1.09
	9	M2"	1.1602	5014.80	1.09
	10	M2"	1.1639	5356.80	1.09
	11	M2"	1.1680	5691.60	1.09
	12	M2"	1.1700	6008.40	1.09
	13	M2"	1.1739	6361.20	1.09
	14	M2"	1.1777	6688.80	1.09
	15	M2"	1.1813	6980.40	1.09
	16	M2"	1.1843	7239.60	1.09
	17	M2"	1.1847	7473.60	1.09
	18	M2"	1.1874	7707.60	1.09
	19	M2"	1.1880	7905.60	1.09
	20	M2"	1.1878	8085.60	1.09
	21	M2"	1.1878	8258.40	1.09
	22	M2"	1.1878	8416.80	1.09
	23	M2"	1.1878	8560.80	1.09
	24	M2"	1.1869	8715.60	1.09
	25	M2"	1.1868	8863.20	1.09
	26	M2"	1.1860	9021.60	1.09
	27	M2"	1.1858	9176.40	1.09
	28	M2"	1.1851	9334.80	1.09
	29	M2"	1.1845	9496.80	1.09
	30	M2"	1.1841	9633.60	1.09
	31	M2"	1.1834	9781.20	1.09
	32	M2"	1.1826	9932.40	1.09
	33	M2"	1.1819	10076.40	1.09
	34	M2"	1.1808	10216.80	1.09
	35	M2"	1.1800	10357.20	1.09
	36	M2"	1.1786	10519.20	1.09
	37	M2"	1.1769	10674.00	1.09
	38	M2"	1.1742	10821.60	1.09
	39	M2"	1.1712	10969.20	1.09
	40	M2"	1.1689	11120.40	1.09
	41	M2"	1.1658	11275.20	1.09
	42	M2"	1.1625	11433.60	1.09
	43	M2"	1.1587	11595.60	1.09
	44	M2"	1.1553	11757.60	1.09
	45	M2"	1.1513	11905.20	1.09
	46	M2"	1.1471	12049.20	1.09
	47	M2"	1.1431	12182.40	1.09
	48	M2"	1.1385	12322.80	1.09
	49	M2"	1.1333	12452.40	1.09
	50	M2"	1.1289	12589.20	1.09
	51	M2"	1.1242	12722.40	1.09

52	M2"	1.1188	12862.80	1.09
53	M2"	1.1122	12992.40	1.09
54	M2"	1.1070	13125.60	1.09
55	M2"	1.1009	13266.00	1.09
56	M2"	1.0955	13410.00	1.09
57	M2"	1.0887	13557.60	1.09
58	M2"	1.0810	13701.60	1.09
59	M2"	1.0735	13852.80	1.09
60	M2"	1.0664	14004.00	1.09
61	M2"	1.0576	14155.20	1.09
62	M2"	1.0496	14313.60	1.09
63	M2"	1.0406	14475.60	1.09
64	M2"	1.0314	14641.20	1.09
65	M2"	1.0217	14817.60	1.09
66	M2"	1.0119	15001.20	1.09
67	M2"	1.0011	15177.60	1.09
68	M2"	0.9912	15350.40	1.09
69	M2"	0.9807	15548.40	1.09
70	M2"	0.9709	15757.20	1.09
71	M2"	0.9586	15984.00	1.09
72	M2"	0.9469	16214.40	1.09
73	M2"	0.9352	16452.00	1.09
74	M2"	0.9242	16671.60	1.09
75	M2"	0.9131	16894.80	1.09
76	M2"	0.9027	17107.20	1.09
77	M2"	0.8920	17373.60	1.09
78	M2"	0.8812	17640.00	1.09
79	M2"	0.8719	17895.60	1.09
80	M2"	0.8603	18190.80	1.09
81	M2"	0.8526	18435.60	1.09
82	M2"	0.8441	18723.60	1.09
83	M2"	0.8364	19011.60	1.09
84	M2"	0.8355	19346.40	1.09
85	M2"	0.8289	19681.20	1.09
86	M2"	0.8288	20739.60	1.09
87	M2"	0.8229	21787.20	1.09
88	M2"	0.8215	22122.00	1.09
89	M2"	0.8152	22395.60	1.09
90	M2"	0.8115	22672.80	1.09

Card Image 20

C20 IPBW	JPBW	ISPBW	NPFORW	NPSERW
2	2	0	1	0
2	3	0	2	0
2	4	0	3	0
2	5	0	4	0
2	6	0	5	0
2	7	0	6	0
2	8	0	7	0
2	9	0	8	0
2	10	0	9	0
2	11	0	10	0

2	12	0	11	0
2	13	0	12	0
2	14	0	13	0
2	15	0	14	0
2	16	0	15	0
2	17	0	16	0
2	18	0	17	0
2	19	0	18	0
2	20	0	19	0
2	21	0	20	0
2	22	0	21	0
2	23	0	22	0
2	24	0	23	0
2	25	0	24	0
2	26	0	25	0
2	27	0	26	0
2	28	0	27	0
2	29	0	28	0
2	30	0	29	0
2	31	0	30	0
2	32	0	31	0
2	33	0	32	0
2	34	0	33	0
2	35	0	34	0
2	36	0	35	0
2	37	0	36	0
2	38	0	37	0
2	39	0	38	0
2	40	0	39	0
2	41	0	40	0
2	42	0	41	0
2	43	0	42	0
2	44	0	43	0
2	45	0	44	0
2	46	0	45	0
2	47	0	46	0
2	48	0	47	0
2	49	0	48	0
2	50	0	49	0
2	51	0	50	0
2	52	0	51	0
2	53	0	52	0
2	54	0	53	0
2	55	0	54	0
2	56	0	55	0
2	57	0	56	0
2	58	0	57	0
2	59	0	58	0
2	60	0	59	0
2	61	0	60	0
2	62	0	61	0
2	63	0	62	0
2	64	0	63	0
2	65	0	64	0
2	66	0	65	0
2	67	0	66	0
2	68	0	67	0

2	69	0	68	0
2	70	0	69	0
2	71	0	70	0
2	72	0	71	0
2	73	0	72	0
2	74	0	73	0
2	75	0	74	0
2	76	0	75	0
2	77	0	76	0
2	78	0	77	0
2	79	0	78	0
2	80	0	79	0
2	81	0	80	0
2	82	0	81	0
2	83	0	82	0
2	84	0	83	0
2	85	0	84	0
2	86	0	85	0
2	89	0	86	0
2	92	0	87	0
2	93	0	88	0
2	94	0	89	0
2	95	0	90	0

Card images 14 through 22 provide basic data for specifying periodic water surface elevation forcings on open boundaries as well as controlling in place least squares harmonic analysis of modeling predictions. MTIDE specifies the number of periodic constituents. In this study only M2 tide was considered. ISLSHA=1 activates the least squares harmonic analysis at MLLSHA (= 8) user specified horizontal locations (given in Card 16) over NTCLSHA reference time periods. The analysis assumes a steady component or a linear trend component if ISLSRT is set to 1. The switch ISHTA should only be activated if MTIDE is equal to 1, with a single period constituent least squares harmonic analysis activated for the entire free surface displacement and horizontal velocity field. Card image 15 specifies user defined symbols or standard NOAA tidal constituent symbols and forcing periods for the MTIDE constituents. In Card 16, the following four switches activate the analysis for surface elevation, salinity, the barotropic or depth integrated horizontal velocity and the horizontal velocity in each layers. The character string identifies the analysis location. Card image 17 specifies the number of open boundary cells on south, west (= 90), east and north open boundaries in the computational grid, as well as the number of periodic forcing functions, the number of surface elevation time series to be used for open boundary forcings and an initial

adjustment to the water surface elevation. The western boundary condition was specified in Card 20.

Card Image 23

C23	NVBS	NUBW	NUBE	NVBN	NQSIJ	NQSER	NQCTL	NQWR	ISDIQ
	0	0	0	0	4	0	0	0	0

Card Image 24

IQS	JQS	QSSE	NQSMUL	NQSMFF	NQSERQ	NS-	NT-	ND-	NSD-	NSN-	NTX-	NSF-
76	73	2378	0	0	0	0	0	0	0	0	0	0
76	72	1378	0	0	0	0	0	0	0	0	0	0
67	82	1378	0	0	0	0	0	0	0	0	0	0
67	80	2378	0	0	0	0	0	0	0	0	0	0

Card Image 25

C25	SALT	TEMP	DYEC	SEDC	SNDC	TOXC	SFLC
	0.	25.	0.	20.	0.	0.	0.
	0.	25.	0.	20.	0.	0.	0.
	0.	25.	0.	20.	0.	0.	0.
	0.	25.	0.	20.	0.	0.	0.

Card images 23 through 25 specify basic information on volumetric sources and sinks. Total 4 point sources (NQSIJ) were picked at locations in Han River given by Card 24. Constant flow rates were given by QSSE. Fresh water inflow with 20 mg/l and 25 °C was assumed (Card 25).

Card Image 29

SEDO	SEDBO	SDEN	SSG	WSEDO	SEDN	SEXP	TAUD	WRSPO	TAUR	TAUN	TEX	SDBLV
20.0	0.	0.0	2.5	5.E-5	1.E-5	0.	7.5E-5	0.2	1.E-4	1.E-4	1.	0.

Card image 29 specifies information for the transport of suspended cohesive sediment.

Card Image 30A

C30A	BSC	TEMO	HEQT	RKDYE	TOXINIT	TOXBINIT	TOXPAR	RKTOX
	1.	25.0	0.0	0.0	0.0	0.0	0.05	0.

Card image 30A includes concentration parameters for buoy, eq temp, dye decay and toxic contaminants. Here, we consider buoyancy effect (BSC = 1).

Card Image 30B

C30B	NCBS	NCBW	NCBE	NCBN	NSSER	NTSER	NDSER	NSDSER	NSNSER	NTXSER	NSFSER
	0	90	0	0	0	0	0	0	0	0	0

Card Image 34

IBBW	JBBW	NTSCRW	NSSERW	NTSERW	NDSERW	NSDSERW	NSNSERW	NTXSERW	NSFSERW
2	2	30	0	0	0	0	0	0	0
2	3	30	0	0	0	0	0	0	0
2	4	30	0	0	0	0	0	0	0
2	5	30	0	0	0	0	0	0	0
2	6	30	0	0	0	0	0	0	0
2	7	30	0	0	0	0	0	0	0
2	8	30	0	0	0	0	0	0	0
2	9	30	0	0	0	0	0	0	0
2	10	30	0	0	0	0	0	0	0
2	11	30	0	0	0	0	0	0	0
2	12	30	0	0	0	0	0	0	0
2	13	30	0	0	0	0	0	0	0
2	14	30	0	0	0	0	0	0	0
2	15	30	0	0	0	0	0	0	0
2	16	30	0	0	0	0	0	0	0
2	17	30	0	0	0	0	0	0	0
2	18	30	0	0	0	0	0	0	0
2	19	30	0	0	0	0	0	0	0
2	20	30	0	0	0	0	0	0	0
2	21	30	0	0	0	0	0	0	0
2	22	30	0	0	0	0	0	0	0
2	23	30	0	0	0	0	0	0	0
2	24	30	0	0	0	0	0	0	0
2	25	30	0	0	0	0	0	0	0
2	26	30	0	0	0	0	0	0	0
2	27	30	0	0	0	0	0	0	0
2	28	30	0	0	0	0	0	0	0
2	29	30	0	0	0	0	0	0	0
2	30	30	0	0	0	0	0	0	0
2	31	30	0	0	0	0	0	0	0
2	32	30	0	0	0	0	0	0	0

2	33	30	0	0	0	0	0	0	0
2	34	30	0	0	0	0	0	0	0
2	35	30	0	0	0	0	0	0	0
2	36	30	0	0	0	0	0	0	0
2	37	30	0	0	0	0	0	0	0
2	38	30	0	0	0	0	0	0	0
2	39	30	0	0	0	0	0	0	0
2	40	30	0	0	0	0	0	0	0
2	41	30	0	0	0	0	0	0	0
2	42	30	0	0	0	0	0	0	0
2	43	30	0	0	0	0	0	0	0
2	44	30	0	0	0	0	0	0	0
2	45	30	0	0	0	0	0	0	0
2	46	30	0	0	0	0	0	0	0
2	47	30	0	0	0	0	0	0	0
2	48	30	0	0	0	0	0	0	0
2	49	30	0	0	0	0	0	0	0
2	50	30	0	0	0	0	0	0	0
2	51	30	0	0	0	0	0	0	0
2	52	30	0	0	0	0	0	0	0
2	53	30	0	0	0	0	0	0	0
2	54	30	0	0	0	0	0	0	0
2	55	30	0	0	0	0	0	0	0
2	56	30	0	0	0	0	0	0	0
2	57	30	0	0	0	0	0	0	0
2	58	30	0	0	0	0	0	0	0
2	59	30	0	0	0	0	0	0	0
2	60	30	0	0	0	0	0	0	0
2	61	30	0	0	0	0	0	0	0
2	62	30	0	0	0	0	0	0	0
2	63	30	0	0	0	0	0	0	0
2	64	30	0	0	0	0	0	0	0
2	65	30	0	0	0	0	0	0	0
2	66	30	0	0	0	0	0	0	0
2	67	30	0	0	0	0	0	0	0
2	68	30	0	0	0	0	0	0	0
2	69	30	0	0	0	0	0	0	0
2	70	30	0	0	0	0	0	0	0
2	71	30	0	0	0	0	0	0	0
2	72	30	0	0	0	0	0	0	0
2	73	30	0	0	0	0	0	0	0
2	74	30	0	0	0	0	0	0	0
2	75	30	0	0	0	0	0	0	0
2	76	30	0	0	0	0	0	0	0
2	77	30	0	0	0	0	0	0	0
2	78	30	0	0	0	0	0	0	0
2	79	30	0	0	0	0	0	0	0
2	80	30	0	0	0	0	0	0	0
2	81	30	0	0	0	0	0	0	0
2	82	30	0	0	0	0	0	0	0
2	83	30	0	0	0	0	0	0	0
2	84	30	0	0	0	0	0	0	0
2	85	30	0	0	0	0	0	0	0
2	86	30	0	0	0	0	0	0	0
2	89	30	0	0	0	0	0	0	0
2	92	30	0	0	0	0	0	0	0
2	93	30	0	0	0	0	0	0	0

2	94	30	0	0	0	0	0	0	0
2	95	30	0	0	0	0	0	0	0

Card Image 35

C35 SALT	TEMP	DYEC	SEDC	SNDC	TOXC	SFLC
30.	25.	0.	0.	0.	0.	0.
30.	25.	0.	0.	0.	0.	0.
30.	25.	0.	0.	0.	0.	0.
30.	25.	0.	0.	0.	0.	0.
30.	25.	0.	0.	0.	0.	0.
30.	25.	0.	0.	0.	0.	0.
30.	25.	0.	0.	0.	0.	0.
30.	25.	0.	0.	0.	0.	0.
30.	25.	0.	0.	0.	0.	0.
30.	25.	0.	0.	0.	0.	0.
30.	25.	0.	0.	0.	0.	0.
30.	25.	0.	0.	0.	0.	0.
30.	25.	0.	0.	0.	0.	0.
30.	25.	0.	0.	0.	0.	0.
30.	25.	0.	0.	0.	0.	0.
30.	25.	0.	0.	0.	0.	0.
30.	25.	0.	0.	0.	0.	0.
30.	25.	0.	0.	0.	0.	0.
30.	25.	0.	0.	0.	0.	0.
30.	25.	0.	0.	0.	0.	0.
30.	25.	0.	0.	0.	0.	0.
30.	25.	0.	0.	0.	0.	0.
30.	25.	0.	0.	0.	0.	0.
30.	25.	0.	0.	0.	0.	0.
30.	25.	0.	0.	0.	0.	0.
30.	25.	0.	0.	0.	0.	0.
30.	25.	0.	0.	0.	0.	0.
30.	25.	0.	0.	0.	0.	0.
30.	25.	0.	0.	0.	0.	0.
30.	25.	0.	0.	0.	0.	0.
30.	25.	0.	0.	0.	0.	0.
30.	25.	0.	0.	0.	0.	0.
30.	25.	0.	0.	0.	0.	0.
30.	25.	0.	0.	0.	0.	0.
30.	25.	0.	0.	0.	0.	0.
30.	25.	0.	0.	0.	0.	0.
30.	25.	0.	0.	0.	0.	0.
30.	25.	0.	0.	0.	0.	0.
30.	25.	0.	0.	0.	0.	0.
30.	25.	0.	0.	0.	0.	0.
30.	25.	0.	0.	0.	0.	0.
30.	25.	0.	0.	0.	0.	0.
30.	25.	0.	0.	0.	0.	0.
30.	25.	0.	0.	0.	0.	0.
30.	25.	0.	0.	0.	0.	0.
30.	25.	0.	0.	0.	0.	0.
30.	25.	0.	0.	0.	0.	0.
30.	25.	0.	0.	0.	0.	0.
30.	25.	0.	0.	0.	0.	0.
30.	25.	0.	0.	0.	0.	0.

```
          30.  25.     0.   0.    0.   0.    0.
          30.  25.     0.   0.    0.   0.    0.
          30.  25.     0.   0.    0.   0.    0.
          30.  25.     0.   0.    0.   0.    0.
          30.  25.     0.   0.    0.   0.    0.
          30.  25.     0.   0.    0.   0.    0.
          30.  25.     0.   0.    0.   0.    0.
          30.  25.     0.   0.    0.   0.    0.
          30.  25.     0.   0.    0.   0.    0.
          30.  25.     0.   0.    0.   0.    0.
          30.  25.     0.   0.    0.   0.    0.
          30.  25.     0.   0.    0.   0.    0.
          30.  25.     0.   0.    0.   0.    0.
          30.  25.     0.   0.    0.   0.    0.
          30.  25.     0.   0.    0.   0.    0.
          30.  25.     0.   0.    0.   0.    0.
          30.  25.     0.   0.    0.   0.    0.
          30.  25.     0.   0.    0.   0.    0.
          30.  25.     0.   0.    0.   0.    0.
          30.  25.     0.   0.    0.   0.    0.
          30.  25.     0.   0.    0.   0.    0.
          30.  25.     0.   0.    0.   0.    0.
          30.  25.     0.   0.    0.   0.    0.
          30.  25.     0.   0.    0.   0.    0.
          30.  25.     0.   0.    0.   0.    0.
          30.  25.     0.   0.    0.   0.    0.
          30.  25.     0.   0.    0.   0.    0.
          30.  25.     0.   0.    0.   0.    0.
          30.  25.     0.   0.    0.   0.    0.
          30.  25.     0.   0.    0.   0.    0.
          30.  25.     0.   0.    0.   0.    0.
          30.  25.     0.   0.    0.   0.    0.
          30.  25.     0.   0.    0.   0.    0.
          30.  25.     0.   0.    0.   0.    0.
          30.  25.     0.   0.    0.   0.    0.
          30.  25.     0.   0.    0.   0.    0.
          30.  25.     0.   0.    0.   0.    0.
          30.  25.     0.   0.    0.   0.    0.
          30.  25.     0.   0.    0.   0.    0.
          30.  25.     0.   0.    0.   0.    0.
```

Card Image 36

```
C36 SALT  TEMP  DYEC  SEDC   SNDC  TOXC  SFLC
          30.  25.     0.   0.    0.   0.    0.
          30.  25.     0.   0.    0.   0.    0.
          30.  25.     0.   0.    0.   0.    0.
          30.  25.     0.   0.    0.   0.    0.
          30.  25.     0.   0.    0.   0.    0.
          30.  25.     0.   0.    0.   0.    0.
          30.  25.     0.   0.    0.   0.    0.
          30.  25.     0.   0.    0.   0.    0.
          30.  25.     0.   0.    0.   0.    0.
          30.  25.     0.   0.    0.   0.    0.
          30.  25.     0.   0.    0.   0.    0.
          30.  25.     0.   0.    0.   0.    0.
```

30.	25.	0.	0.	0.	0.	0.
30.	25.	0.	0.	0.	0.	0.
30.	25.	0.	0.	0.	0.	0.
30.	25.	0.	0.	0.	0.	0.
30.	25.	0.	0.	0.	0.	0.
30.	25.	0.	0.	0.	0.	0.
30.	25.	0.	0.	0.	0.	0.
30.	25.	0.	0.	0.	0.	0.
30.	25.	0.	0.	0.	0.	0.
30.	25.	0.	0.	0.	0.	0.
30.	25.	0.	0.	0.	0.	0.
30.	25.	0.	0.	0.	0.	0.
30.	25.	0.	0.	0.	0.	0.
30.	25.	0.	0.	0.	0.	0.
30.	25.	0.	0.	0.	0.	0.
30.	25.	0.	0.	0.	0.	0.
30.	25.	0.	0.	0.	0.	0.
30.	25.	0.	0.	0.	0.	0.
30.	25.	0.	0.	0.	0.	0.
30.	25.	0.	0.	0.	0.	0.
30.	25.	0.	0.	0.	0.	0.
30.	25.	0.	0.	0.	0.	0.
30.	25.	0.	0.	0.	0.	0.
30.	25.	0.	0.	0.	0.	0.
30.	25.	0.	0.	0.	0.	0.
30.	25.	0.	0.	0.	0.	0.
30.	25.	0.	0.	0.	0.	0.
30.	25.	0.	0.	0.	0.	0.
30.	25.	0.	0.	0.	0.	0.
30.	25.	0.	0.	0.	0.	0.
30.	25.	0.	0.	0.	0.	0.
30.	25.	0.	0.	0.	0.	0.
30.	25.	0.	0.	0.	0.	0.
30.	25.	0.	0.	0.	0.	0.
30.	25.	0.	0.	0.	0.	0.
30.	25.	0.	0.	0.	0.	0.
30.	25.	0.	0.	0.	0.	0.
30.	25.	0.	0.	0.	0.	0.
30.	25.	0.	0.	0.	0.	0.
30.	25.	0.	0.	0.	0.	0.
30.	25.	0.	0.	0.	0.	0.
30.	25.	0.	0.	0.	0.	0.
30.	25.	0.	0.	0.	0.	0.
30.	25.	0.	0.	0.	0.	0.
30.	25.	0.	0.	0.	0.	0.
30.	25.	0.	0.	0.	0.	0.
30.	25.	0.	0.	0.	0.	0.
30.	25.	0.	0.	0.	0.	0.
30.	25.	0.	0.	0.	0.	0.
30.	25.	0.	0.	0.	0.	0.
30.	25.	0.	0.	0.	0.	0.
30.	25.	0.	0.	0.	0.	0.
30.	25.	0.	0.	0.	0.	0.
30.	25.	0.	0.	0.	0.	0.
30.	25.	0.	0.	0.	0.	0.
30.	25.	0.	0.	0.	0.	0.
30.	25.	0.	0.	0.	0.	0.

```
30.  25.    0.  0.   0.  0.   0.
30.  25.    0.  0.   0.  0.   0.
30.  25.    0.  0.   0.  0.   0.
30.  25.    0.  0.   0.  0.   0.
30.  25.    0.  0.   0.  0.   0.
30.  25.    0.  0.   0.  0.   0.
30.  25.    0.  0.   0.  0.   0.
30.  25.    0.  0.   0.  0.   0.
30.  25.    0.  0.   0.  0.   0.
30.  25.    0.  0.   0.  0.   0.
30.  25.    0.  0.   0.  0.   0.
30.  25.    0.  0.   0.  0.   0.
30.  25.    0.  0.   0.  0.   0.
30.  25.    0.  0.   0.  0.   0.
30.  25.    0.  0.   0.  0.   0.
30.  25.    0.  0.   0.  0.   0.
30.  25.    0.  0.   0.  0.   0.
30.  25.    0.  0.   0.  0.   0.
30.  25.    0.  0.   0.  0.   0.
30.  25.    0.  0.   0.  0.   0.
30.  25.    0.  0.   0.  0.   0.
```

Card images 30B through 42 specify scalar inflowing concentrations on open boundaries. The western boundary locations given in Card 34 are the same as the tide forcing boundary points given by Card 20. The following Cards 35 and 36 specify time constant inflowing values of salinity, temperature and other transported constituents at bottom and surface, respectively.

Card Image 58

```
C58 ISTMSR   MLTMSR   NBTMSR   NSTMSR   NWTMSR  TCTMSR
      1        15        0     1000000    100    3600.
```

Card Image 59

```
ILTS JLTS  MTSP MTSC MTSA  MTSUE MTSUT MTSU MTSQE MTSQ  CLTS
 53   58    1    1    1     0     0     1     0     0   '53 58 '
 52   58    1    1    1     0     0     1     0     0   '52 58 '
 54   58    1    1    1     0     0     1     0     0   '54 58'
 52   59    1    1    1     0     0     1     0     0   '52 59'
 54   59    1    1    1     0     0     1     0     0   '54 59'
 58   55    1    1    1     0     0     1     0     0   '58 55'
 27   17    1    1    1     0     0     1     0     0   'Kunsan'
 27   41    1    1    1     0     0     1     0     0   'Auhung'
 30   28    1    1    1     0     0     1     0     0   'Wonsando'
```

```
34    53    1     1     1     0     0     1     0     0     'Sungapdo'
 3    87    1     1     1     0     0     1     0     0     'Daechuingdo'
39    56    1     1     1     0     0     1     0     0     'Duckjuckdo'
59    56    1     1     1     0     0     1     0     0     'Inchon 2'
76    72    1     1     1     0     0     1     0     0     'Han r'
67    82    1     1     1     0     0     1     0     0     'up river 2'
```

Card images 58 and 59 control the writing of time series files. Total 15 stations specified in Card 59 were used to retrieve time series output every 100 time steps (= 2 hours). Surface elevation, concentration, eddy viscosity/diffusivity, and horizontal velocities were included in the time series output.

III. Model Results

Figure 3 shows one-day portion of surface elevation time series at the selected cells representing important coastal locations. Propagation of tides from south (Kunsan) to north (Inchon) is apparent. The following table summarizes the tidal range calculated at selected stations compared with existing observations. Reasonable agreement is seen as higher M2 tide range at Inchon (~ 6 m) than at Kunsan (~ 4 m). In Figure 4, phase relationship between current and tide is shown. In general, peak flood current leads high tide. As the tide propagates from south to north, the lag between peak flood and high tide increases. This suggests that the tide becomes characteristically closer to standing wave toward the coastal zone near the Han River entrance. The spatial distribution of surface elevation (Figure 5) shows not only the phase relationships but also the successful implementation of wet-and-dry scheme. The dry cells are represented by gray color. Figure 6 shows the distribution of surface currents varying with changing tidal phase. Typically currents are not in-phase with surface elevations. Under normal condition, the freshwater discharge into the system is small so that the influence of Han River on salinity distribution is limited to the area near its mouth. In order to investigate salinity distribution, finer resolution grid will be needed. To investigate the pollutant transport from Han River, a model simulation of dye release at the upstream end of the Han River was conducted. The simulation result is presented in Figure 7. Water quality was also simulated to test the HEM-3D model. All the conditions were hypothetical. The applicability of the HEM-3D model for water quality study was demonstrated. The results were collected in Appendix B.

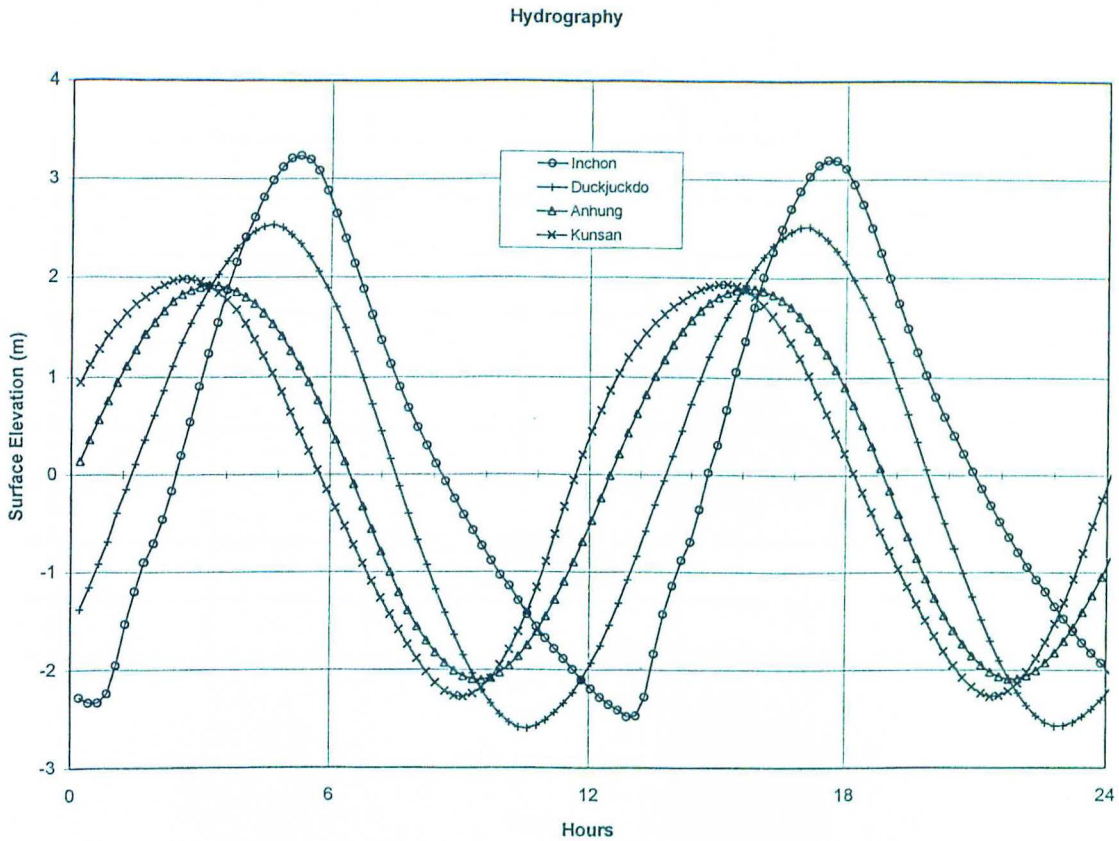

Figure 3. Surface elevation time series at selected stations

Station	Observation (m)	Model (m)	modeled HT lag (hour)	modeled LT lag (hour)
Daechungdo	1.97	2.02	12 .84	11.21
Inchon	5.80	5.73	12.42	12.42
Duckjuckdo	4.94	5.09	11.79	9.94
Sungapdo	4.69	4.54	11.42	9.30
Auhung	4.20	3.99	10.57	8.88
Kunsan	4.20	4.21	9.94	8.46
Wonsando	4.50	4.36	9.73	8.88

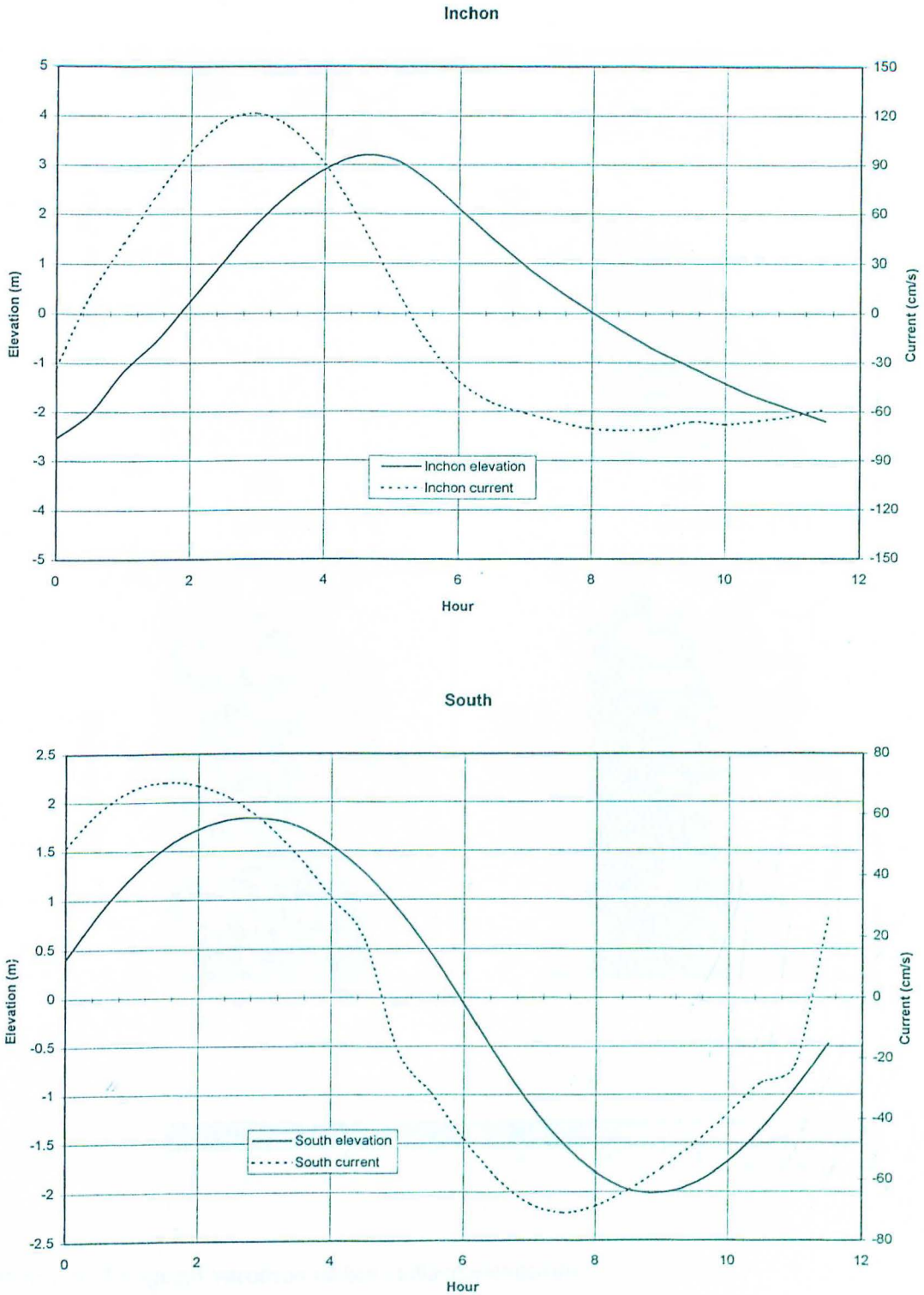

Figure 4. tidal current and elevation at Inchon and southern portion of the model region

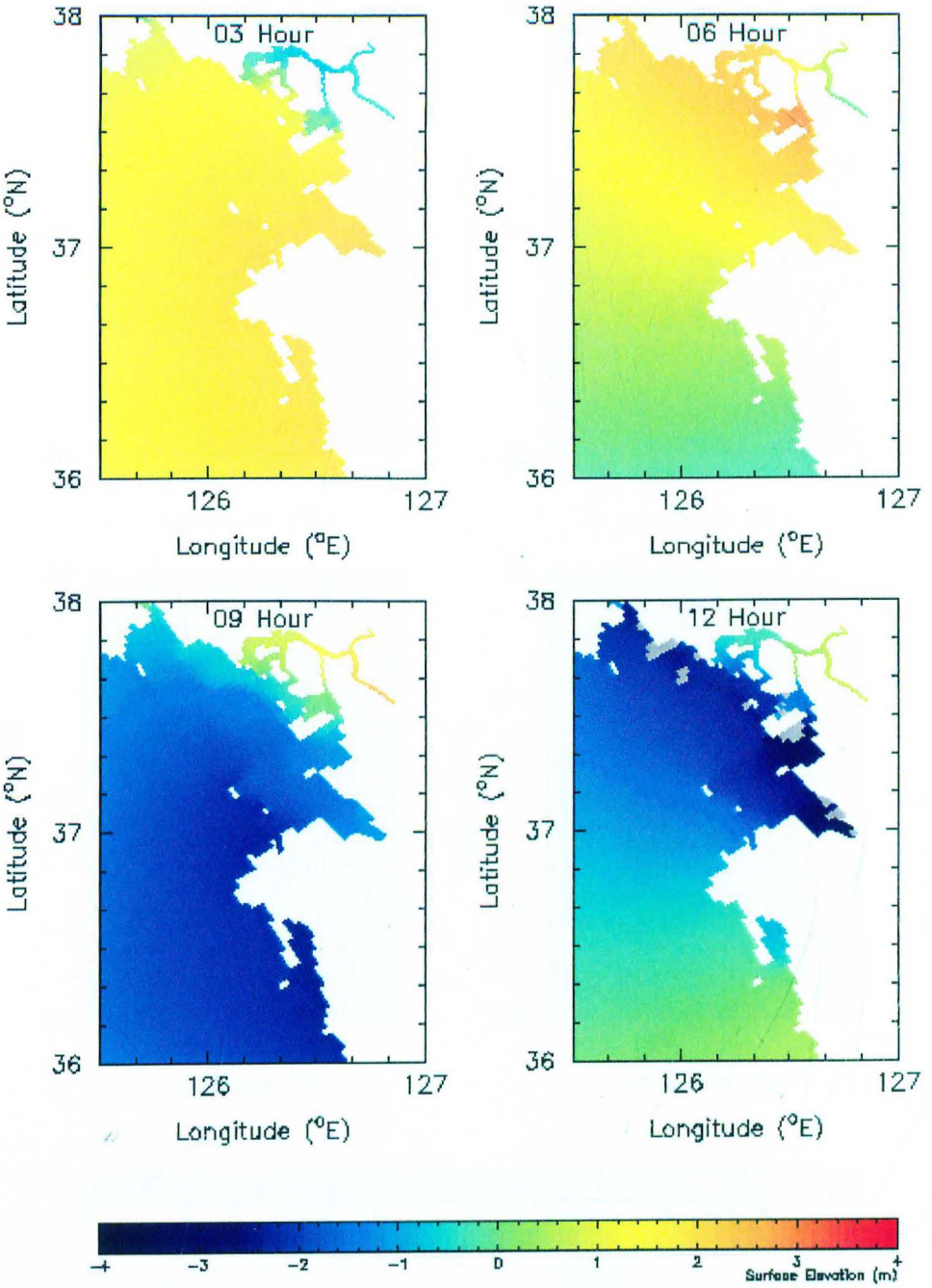

Figure 5. Temporal variation of sea surface elevations

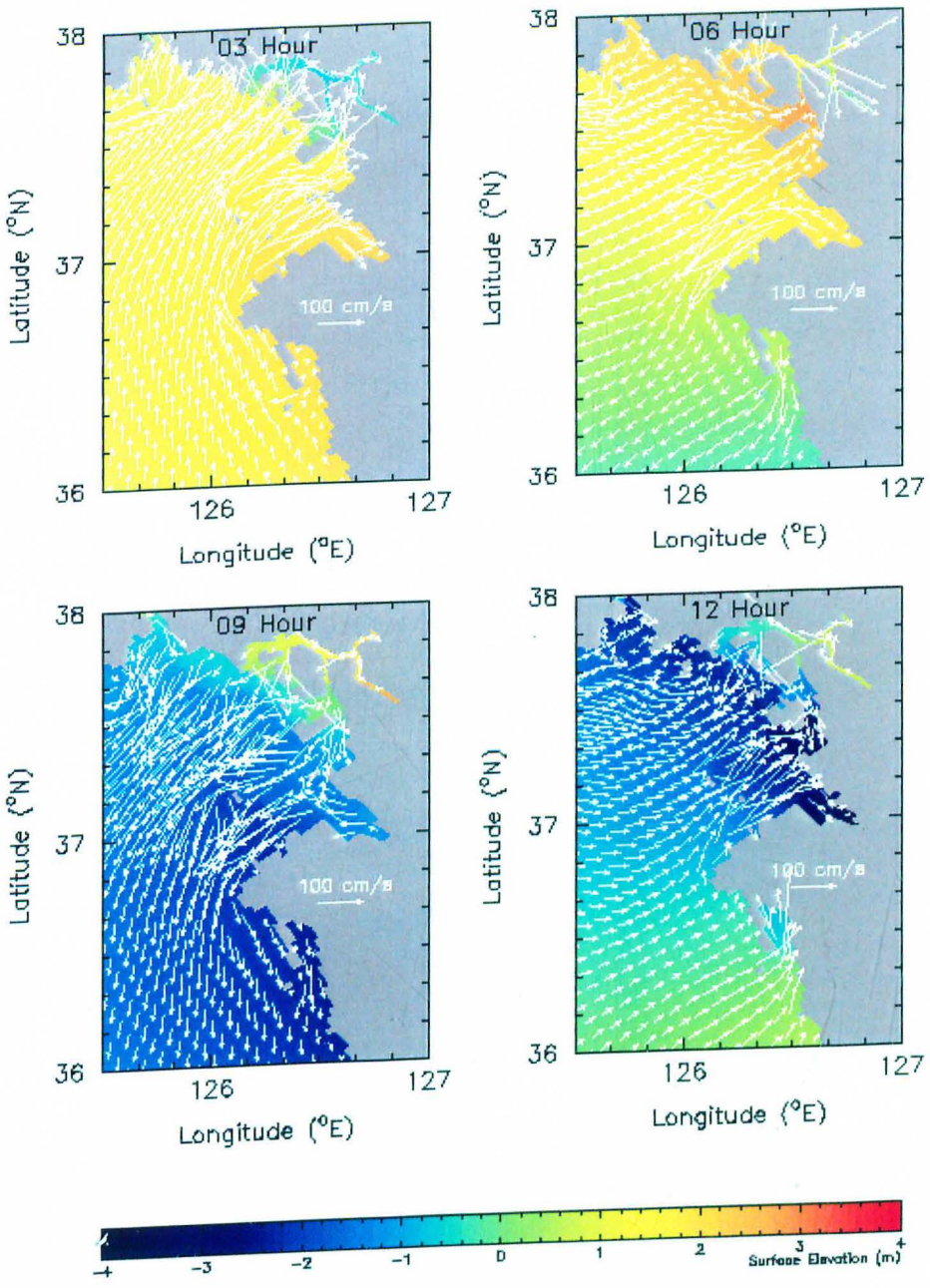

Figure 6. Temporal variation of surface currents with sea surface elevations

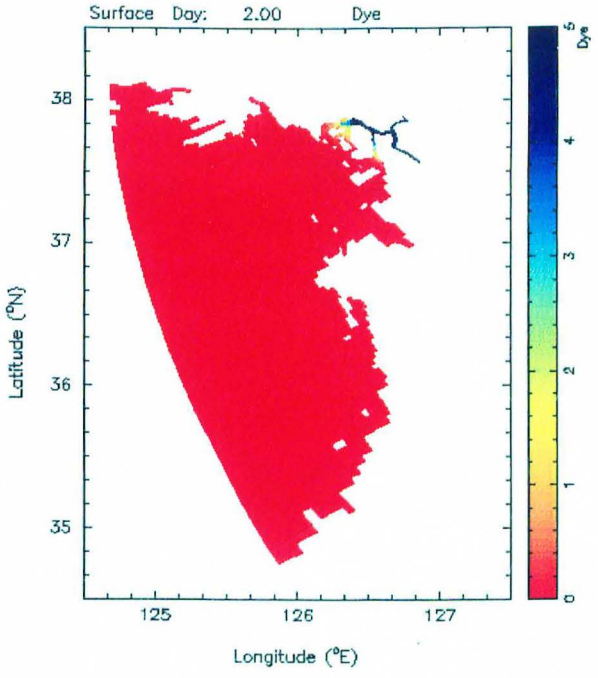

Figure 7a. Dye dispersal pattern (on day 2)

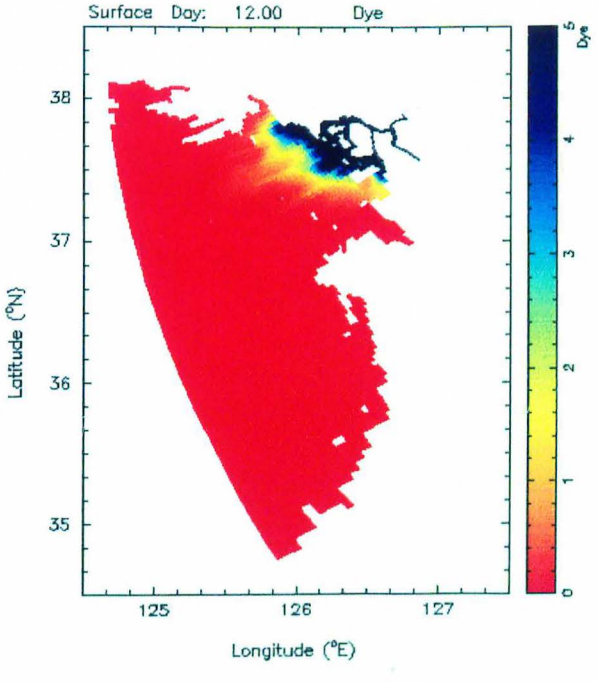

Figure 7b. Dye dispersal pattern (on day 12)

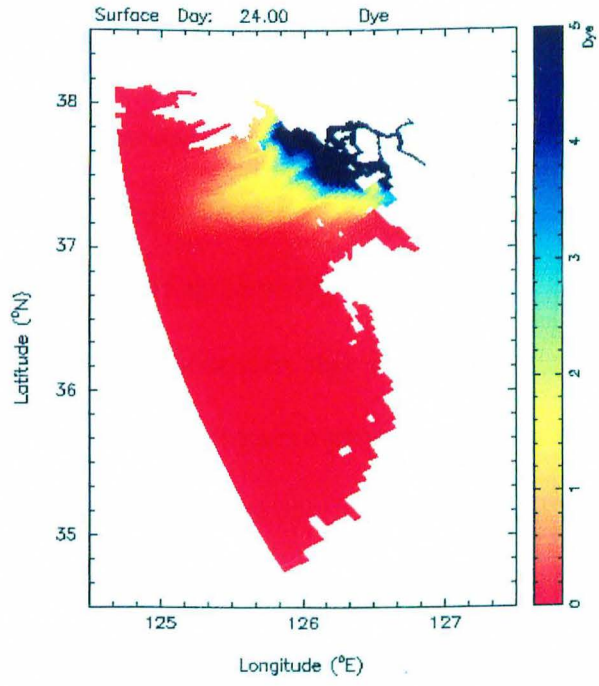

Figure 7c. Dye dispersal pattern (on day 24)

IV. Summary and Conclusions

The HEM-3D model was setup for the Kyunggi Bay, Korea. The model was forced at western open boundary by M2 tide with an amplitude half of mean tidal range. The calculated tidal ranges agree well with available field observations at 7 selected locations. The model results indicate that tidal wave propagates in a general south to north direction. The tidal current has a phase lead with respect to the tidal height. The phase lead increases as the tide approaches the shoreline toward northeast. Since the Kyunggi Bay is a macrotidal sea with extensive subtidal flat, the proper simulation of wet-and-dry cells is of the uttermost importance. The successful calibration with tidal range suggests that the wet-and-dry scheme used in the HEM-3D model is suitable. Under the normal flow condition, the influence of freshwater discharge from the Han River on the salinity distribution is limited to a small area around the river mouth. The grid layout of current model is not fine enough to properly simulate salinity distribution. A higher resolution grid is required. The effluent problem from the Han River was thus investigated with an artificial release of high dose of dye. The resulting dye distribution is quite reasonable in qualitative sense.

Since there is insufficient water quality data for the calibration of water quality portion of the model, the model was run with some hypothetical input conditions. The values of calibration coefficients were based on those of other systems such as the Chesapeake Bay. The results indicate that the model has been properly set up for the Kyunggi Bay. However, the results should be used only for demonstration purpose. It is

LIBRARY of the VIRGINIA INSTITUTE of MARINE SCIENCE

hoped that more water quality and hydrographic data would enhance the operation of the HEM-3D model for the Kyunggi Bay and other coastal waters of Korea.

References

Blumberg, A. F. and G. L. Mellor. 1987. A description of a three-dimensional coastal ocean circulation model. In: Three-Dimensional Coastal and Ocean Models, Coastal and Estuarine Science, Vol. 4. American Geophysical Union, pp. 1-19.

Galperin, B., L. H. Kantha, S. Hassid, and A. Rosati, 1988. A quasi-equilibrium turbulent energy model for geophysical flows. *J. Atmos. Sci.*, **45**, 55-62.

Cerco, C. F., and T. Cole, 1993. Three-dimensional eutrophication model of Chesapeake Bay. *J. Environ. Engnr.*, 119, 1006-1025.

Hamrick, J. M., 1992a. A Three-Dimensional Environmental Fluid Dynamics Computer Code: Theoretical and Computational Aspects. The College of William and Mary, Virginia Institute of Marine Science. Special Report 317, 63 pp.

Hamrick, J. M., 1992b. Estuarine environmental impact assessment using a three-dimensional circulation and transport model. *Estuarine and Coastal Modeling, Proceedings of the 2nd International Conference*, M. L. Spaulding *et al*, Eds., American Society of Civil Engineers, New Yrok, 292-303.

Hamrick, J. M., 1994. Linking hydrodynamic and biogeochemical transport models for estuarine and coastal waters. *Estuarine and Coastal Modeling, Proceedings of the*

3rd International Conference, M. L. Spaulding *et al*, Eds., American Society of Civil Engineers, New York, 591-608.

Hamrick, J. M., A.Y. Kuo, and J. Shen, 1995. Mixing and dilution of the Surry Nuclear Power Plant cooling water discharge into the James River. A report to virginia Power Company, Richmond. The College of William and Mary, Virginia Institute of Marine Science, 76 pp.

Hamrick, J. M. 1996. User's Manual for the Environmental Fluid Dynamics Code. VIMS Special Report in Applied Marine Science and Ocean Engineering # 331. 223 pp.

Kim, S.-C., L.D. Wright, J.P.-Y. Maa, and J. Shen, 1998. Morphodynamic responses to extratropical meteorological forcing on the inner shelf of the Middle Atlantic Bight: wind waves, currents, and suspended sediment transport. (*ed* by M.L. Spaulding and A.F. Blumberg) *Estuarine and coastal modeling, Proceedings of 5th International Conference*, ASCE, 456-466

Mellor, G. L., and T. Yamada, 1982. Development of a turbulence closure model for geophysical fluid problems. *Rev. Geophys. Space Phys.*, **20**, 851-875.

Moustafa, M. Z., and J. M. Hamrick, 1994. Modeling circulation and salinity transport in the Indian River Lagoon. *Estuarine and Coastal Modeling, Proceedings of the*

3rd International Conference, M. L. Spaulding *et al*, Eds., American Society of Civil Engineers, New York, 381-395.

Park, K., A.Y. Kuo, J. Shen, and J.M. Hamrick, 1995. A three-dimensional hydrodynamic-eutrophication model (HEM-3D): Description of water quality and sediment process submodels. VIMS Special Report in Applied Marine Science and Ocean Engineering # 327. 102 pp.

Shen, J., M. Sisson, A. Kuo, J. Boon, and S.-C. Kim, 1998. Three-dimensional numerical modeling of the tidal York River system, Virginia. (*ed* by M.L. Spaulding and A.F. Blumberg) *Estuarine and coastal modeling, Proceedings of 5th International Conference*, ASCE, 495-510

Appendix A. Grid Information file "CELL.INP"

```
C CELL.INP KYUNGGI BAY, KORDI
C-------------1---------2---------3---------4---------5---------6---------7---------8
C     12345678901234567890123456789012345678901234567890123456789012345678901234567890
C
 96   999999999999000000000000000000000000000000000000000000000000000000000000000000000000
 95   955555555599000000000000000000000000000000000000000000000000000000000000000000000000
 94   955555555559900000000000000000000000000000000000000000000000000000000000000000000000
 93   955555555559999999999990000000000000000000000000000000000000000000000000000000000000
 92   955555555555555555555590000000000000000000000000000000000000000000000000000000000000
 91   995555555555555599999990000000000000000000000000000000000000000000000000000000000000
 90   999555555555555599000000000000000000000000000000000000000000000000000000000000000000
 89   955555599999995900000000000000000000000000000000000000000000000000000000000000000000
 88   995555555999999900000000000000000000000000000000000000000000000000000000000000000000
 87   995555555555999900000000000000000000000000000000000000000000000000000000000000000000
 86   955555555555555599999990000000000000009990000000000000000000000000000000000000000000
 85   955555555555555555559000000000000000955900000000000000000000000000000000000000000000
 84   955555555555555559999999999900000000009599000000000000000000000000000000000000000000
 83   955555555555555555555555559000009990099559000000000000000000000000000000000000000000
 82   955555555555555555555555599999995999955590000000000000000000000000000000000000000000
 81   955555555555559999999999999999955555555990000000000000000000000000000000000000000000
 80   955555555555555559999999559999555555555900000000000000000000000000000000000000000000
 79   955555555555555555555555555555955555555590000000000000000000000000000000000000000000
 78   955555555555555555555555555555555555555590000000000000000000000000000000000000000000
 77   955555555555555555555555555555955555555999900000000000000000000000000000000000000000
 76   955555555555555555555555555555955555555599000000000000000000000000000000000000000000
 75   955555555555555555555555555555555555555599000000000000000000000000000000000000000000
 74   955555555555555555555555555555555555555599999999999999999999999999999999999999999999
 73   955555555555555555555555555555555555555599945195455555555555555555555555555555559
 72   955555555555555555555555555555555555555599455555555555555555555555555555555555559
 71   955555555555555555555555555555555555555595559955599959999999999999999999999999999
 70   955555555555555555555555555555555555555595599995900959000000000000000000000000000
 69   955555555555555555555555555555555555555551555555590095900000000000000000000000000
 68   955555555555555555555555555555555555555599959009590095900000000000000000000000000
 67   955555555555555555555555555555555555555595990959009590095900000000000000000000000
 66   955555555555555555555555555555555555555590095900959009590000000000000000000000000
 65   955555555555555555555555555555555555555599995900959009590000000000000000000000000
 64   955555555555555555555555555555555555555590095900959009590000000000000000000000000
 63   955555555555555555555555555555555555555529999009590095900000000000000000000000000
 62   955555555555555555555555555555555555555595519900000959000000000000000000000000000
 61   955555555555555555555555555555555555555595551999999959000000000000000000000000000
 60   955555555555555555555555555555555555555555555555519995900000000000000000000000000
 59   955555555555555555555555555555555555555555555555559000000000000000000000000000000
 58   955555555555555555555555555555555555555555599555555555559000000000000000000000000
 57   955555555555555555555555555555555555555555595555555555559000000000000000000000000
 56   955555555555555555555555555555555555555555555555555555529900000000000000000000000
 55   955555555555555555555555555555555555555955555555555555555529900000000000000000000
 54   955555555555555555555555555555555555555955555555555555555999990000000000000000000
 53   955555555555555555555555555555555555555555555555555555559000000000000000000000000
 52   955555555555555555555555555555555555555555555555555999900000000000000000000000000
 51   955555555555555555555555555555555555555555599555555900000000000000000000000000000
 50   955555555555555555555555555555555555559555555559955559000000000000000000000000000
 49   955555555555555555555555555555555555555555599999990000000000000000000000000000000
 48   955555555555555555555555555555555555555555599900000000000000000000000000000000000
 47   955555555555555555555555555555555555555555599900000000000000000000000000000000000
 46   955555555555555555555555555555595559599555555599000000000000000000000000000000000
 45   955555555555555555555555555555599999599999955551900000000000000000000000000000000
 44   955555555555555555555555555599999999590000955555900000000000000000000000000000000
 43   955555555555555555555555559900000009900009555559000000000000000000000000000000000
 42   955555555555555555555555900000000000009555559000000000000000000000000000000000000
 41   955555555555555555555555990000000000095555590000000000000000000000000000000000000
 40   955555555555555555555555590000000000999559900000000000000000000000000000000000000
 39   955555555555555555555555590000000000095590000000000000000000000000000000000000000
```

```
38  9555555555555555555555555555559000000000000095590000000000000000000000000000000
37  9555555555555555555555555555599990000000000095590000000000000000000000000000000
36  9555555555555555555555555555995999000000000095590000000000000000000000000000000
35  9555555555555555555555555555995519000000000955900000000000000000000000000000000
34  9555555555555555555555555555995559000000000999900000000000000000000000000000000
33  9555555555555555555555555555955559000000000000000000000000000000000000000000000
32  9555555555555555555555555555995559900000000000000000000000000000000000000000000
31  9555555555555555555555555555995559000000000000000000000000000000000000000000000
30  9555555555555555555555555555995599000000000000000000000000000000000000000000000
29  9555555555555555555555555555559000000000000000000000000000000000000000000000000
28  9555555555555555555555555555955599000000000000000000000000000000000000000000000
27  9555555555555555555555555555559000000000000000000000000000000000000000000000000
26  9555555555555555555555555555559000000000000000000000000000000000000000000000000
25  9555555555555555555555555555599000000000000000000000000000000000000000000000000
24  9555555555555555555555555555590000000000000000000000000000000000000000000000000
23  9555555555555555555555555555590000000000000000000000000000000000000000000000000
22  9555555555555555555555555555599000000000000000000000000000000000000000000000000
21  9555555555555555555555555555599000000000000000000000000000000000000000000000000
20  9555555555555555555555555555990000000000000000000000000000000000000000000000000
19  9555555555555555555555555555590000000000000000000000000000000000000000000000000
18  9555555555555555555555555555590000000000000000000000000000000000000000000000000
17  9555555555555555555555555555990000000000000000000000000000000000000000000000000
16  9555555555555555555555555559990000000000000000000000000000000000000000000000000
15  9555555555555555555555559555590000000000000000000000000000000000000000000000000
14  9555555555555555555555555555590000000000000000000000000000000000000000000000000
13  9555555555555599555555559900000000000000000000000000000000000000000000000000000
12  9555555555555555559999990000000000000000000000000000000000000000000000000000000
11  9555555555555555559000000000000000000000000000000000000000000000000000000000000
10  9555555555555555599900000000000000000000000000000000000000000000000000000000000
 9  9555555555555559990000000000000000000000000000000000000000000000000000000000000
 8  9555555555555999000000000000000000000000000000000000000000000000000000000000000
 7  9555595555999900000000000000000000000000000000000000000000000000000000000000000
 6  9555595555900000000000000000000000000000000000000000000000000000000000000000000
 5  9555599995900000000000000000000000000000000000000000000000000000000000000000000
 4  9555590099900000000000000000000000000000000000000000000000000000000000000000000
 3  9559990000000000000000000000000000000000000000000000000000000000000000000000000
 2  9559000000000000000000000000000000000000000000000000000000000000000000000000000
 1  9999000000000000000000000000000000000000000000000000000000000000000000000000000
```

Appendix B. Water quality simulations

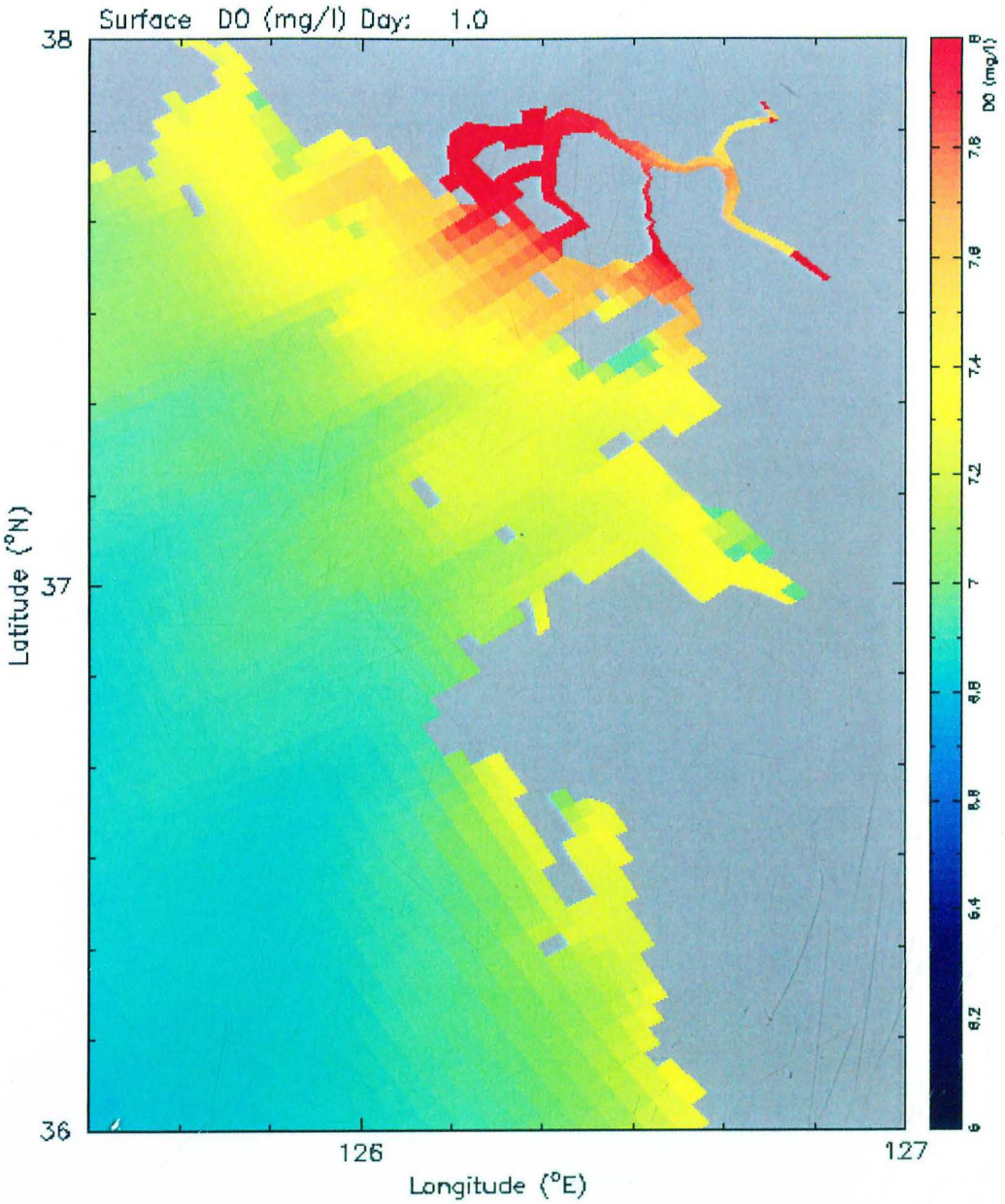

Figure A1. Surface DO (mg/l) at day 1

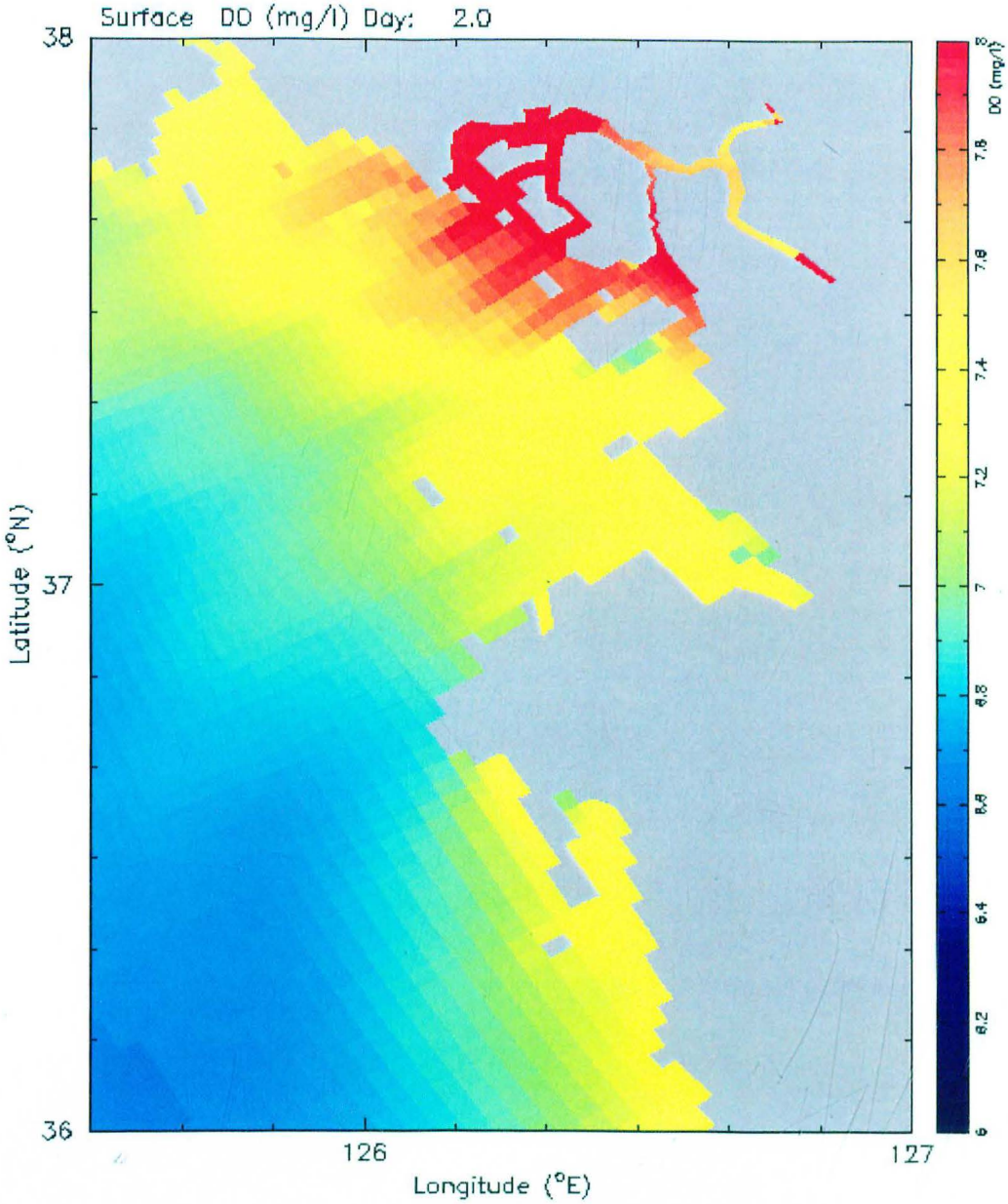

Figure A2. Surface DO (mg/l) at day 2

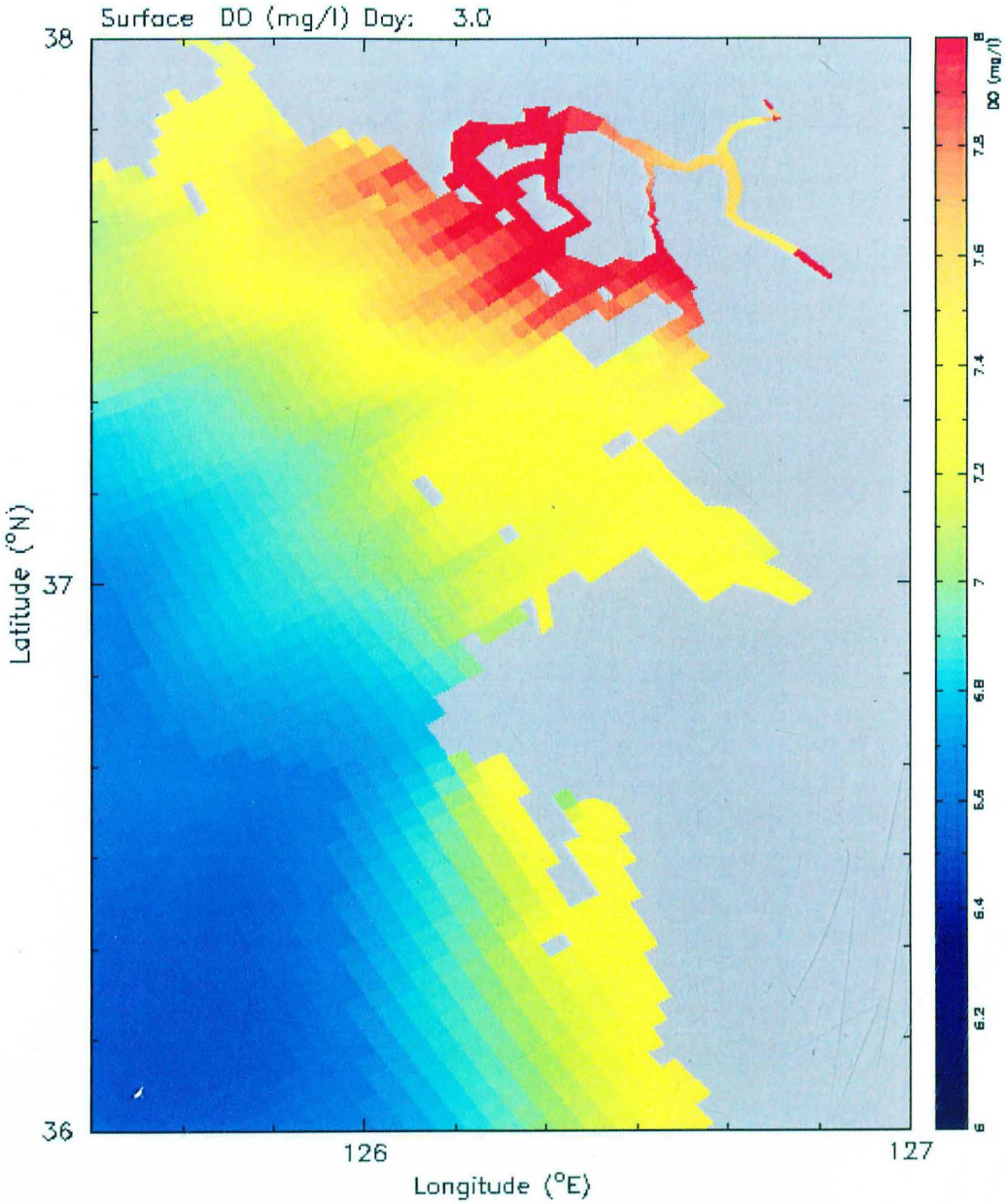

Figure A3. Surface DO (mg/l) at day 3

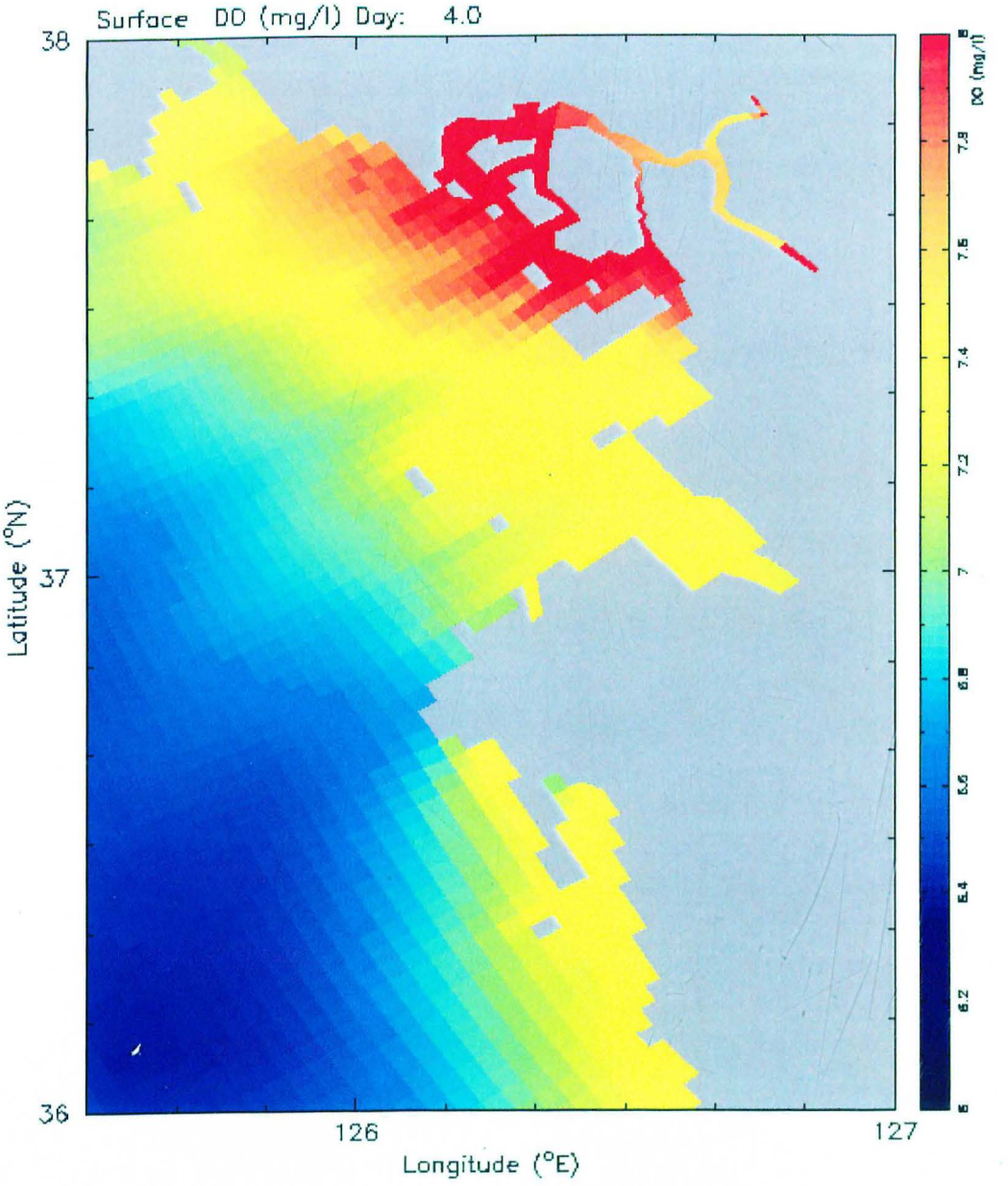

Figure A4. Surface DO (mg/l) at day 4

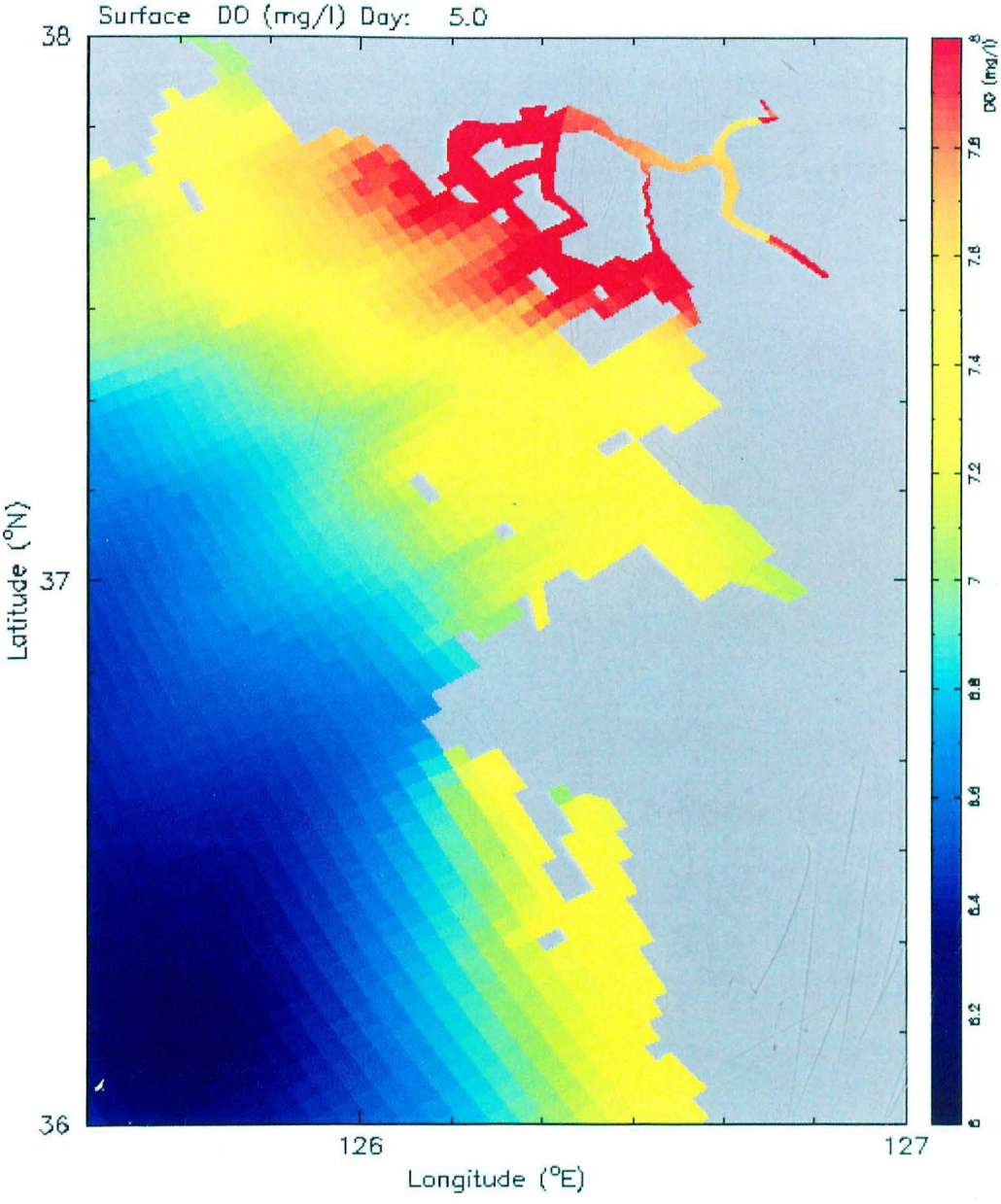

Figure A5. Surface DO (mg/l) at day 5

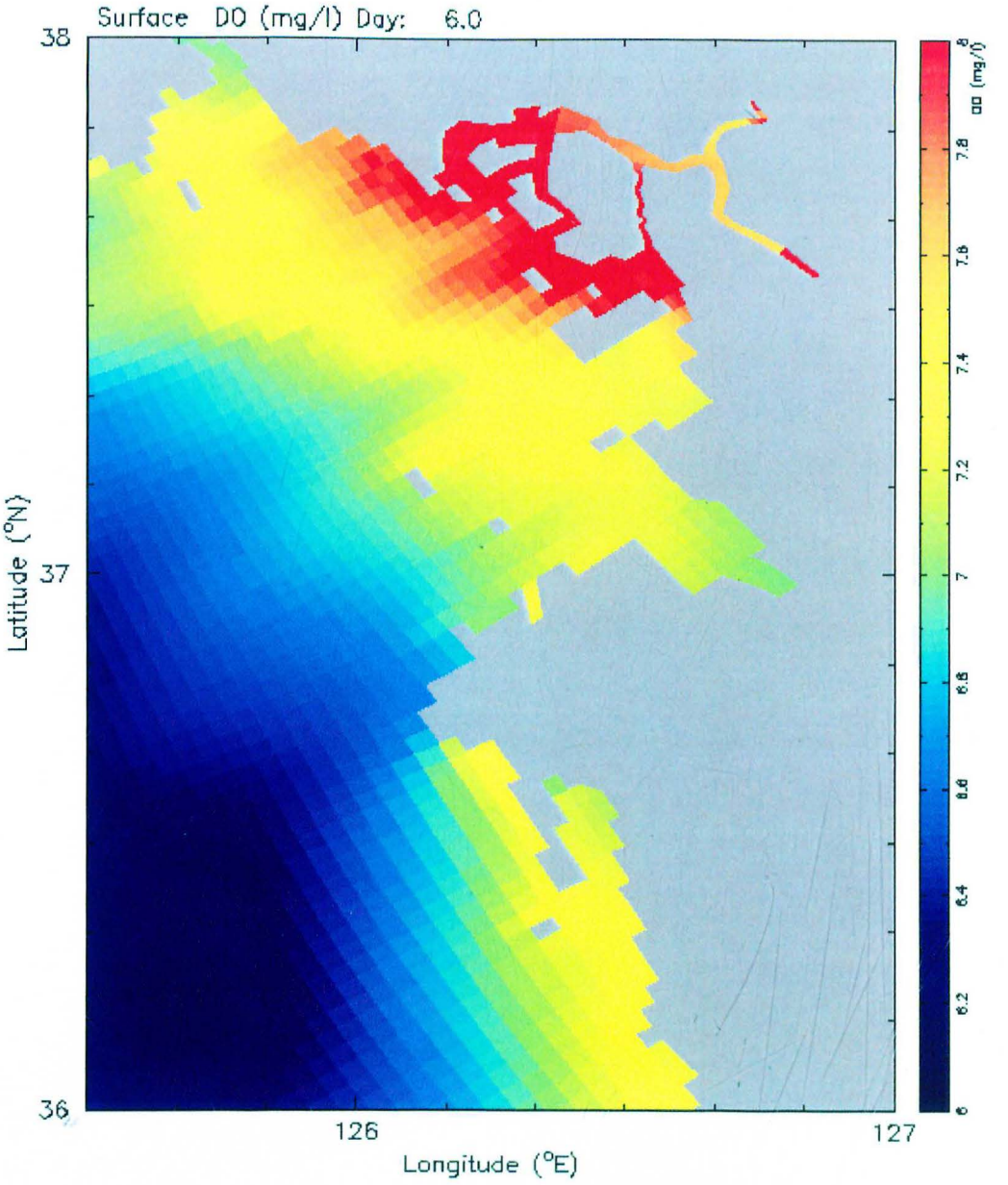

Figure A6. Surface DO (mg/l) at day 6

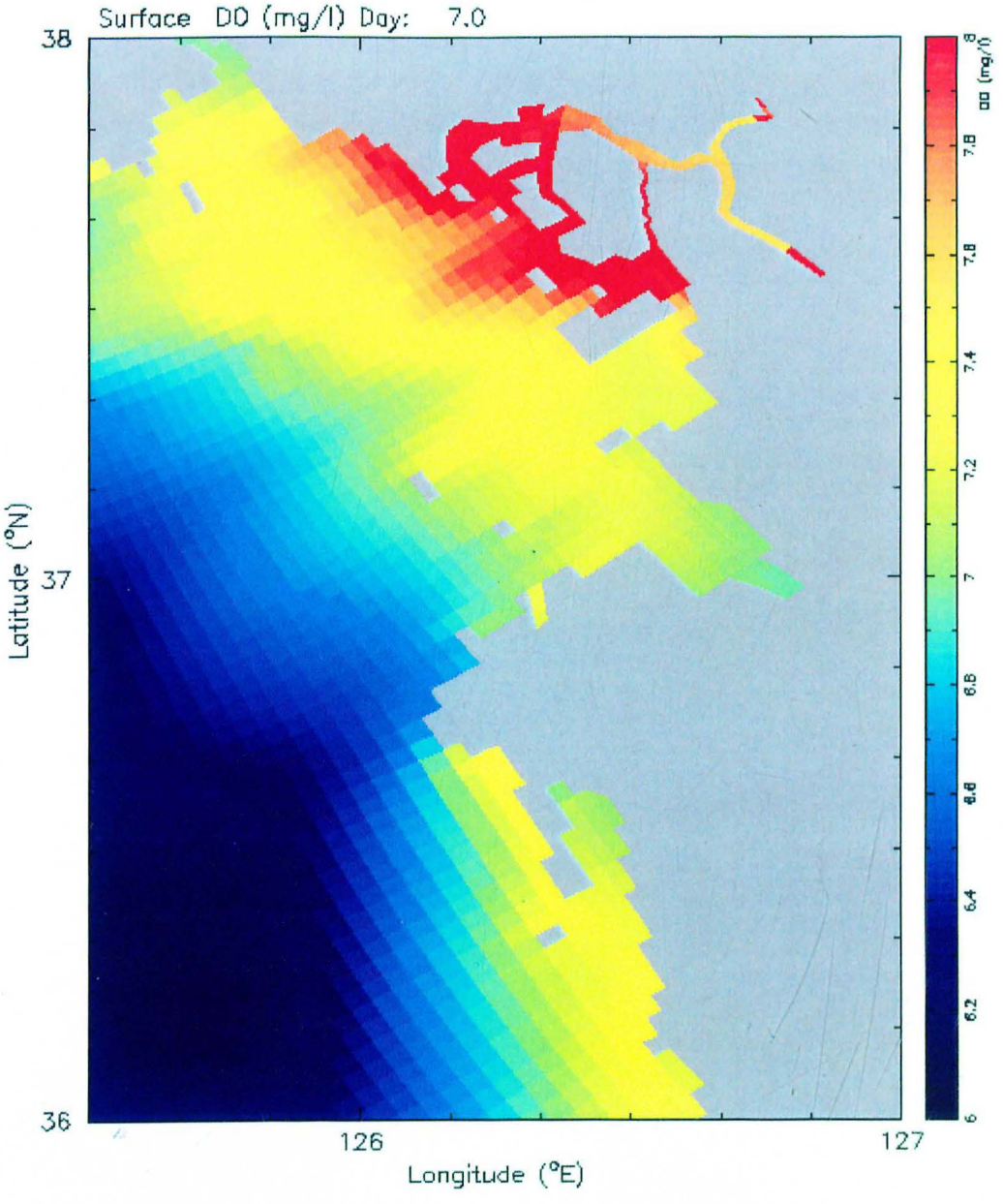

Figure A7. Surface DO (mg/l) at day 7

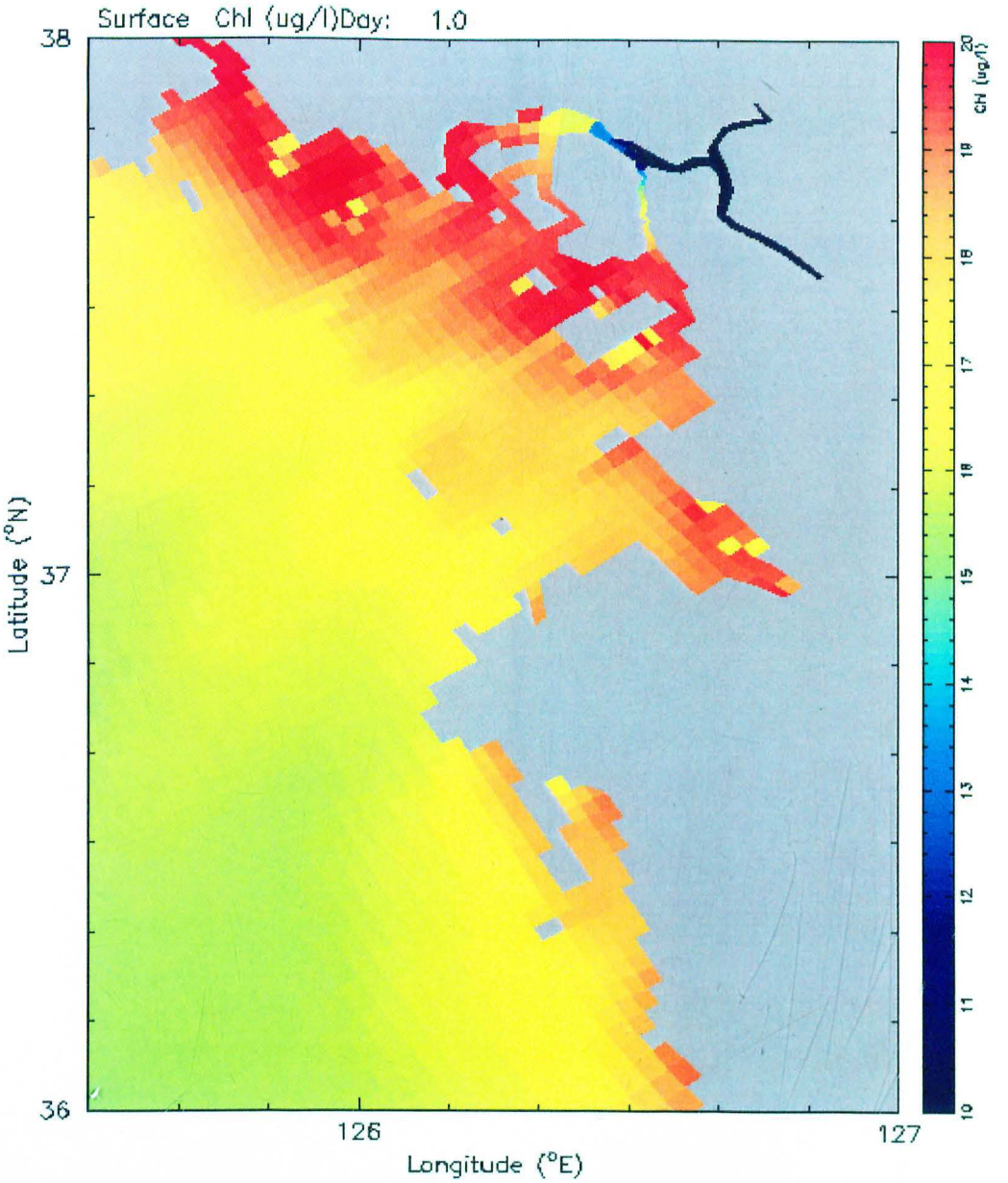

Figure A8. Surface Chlorophyll (µg/l) at day 1

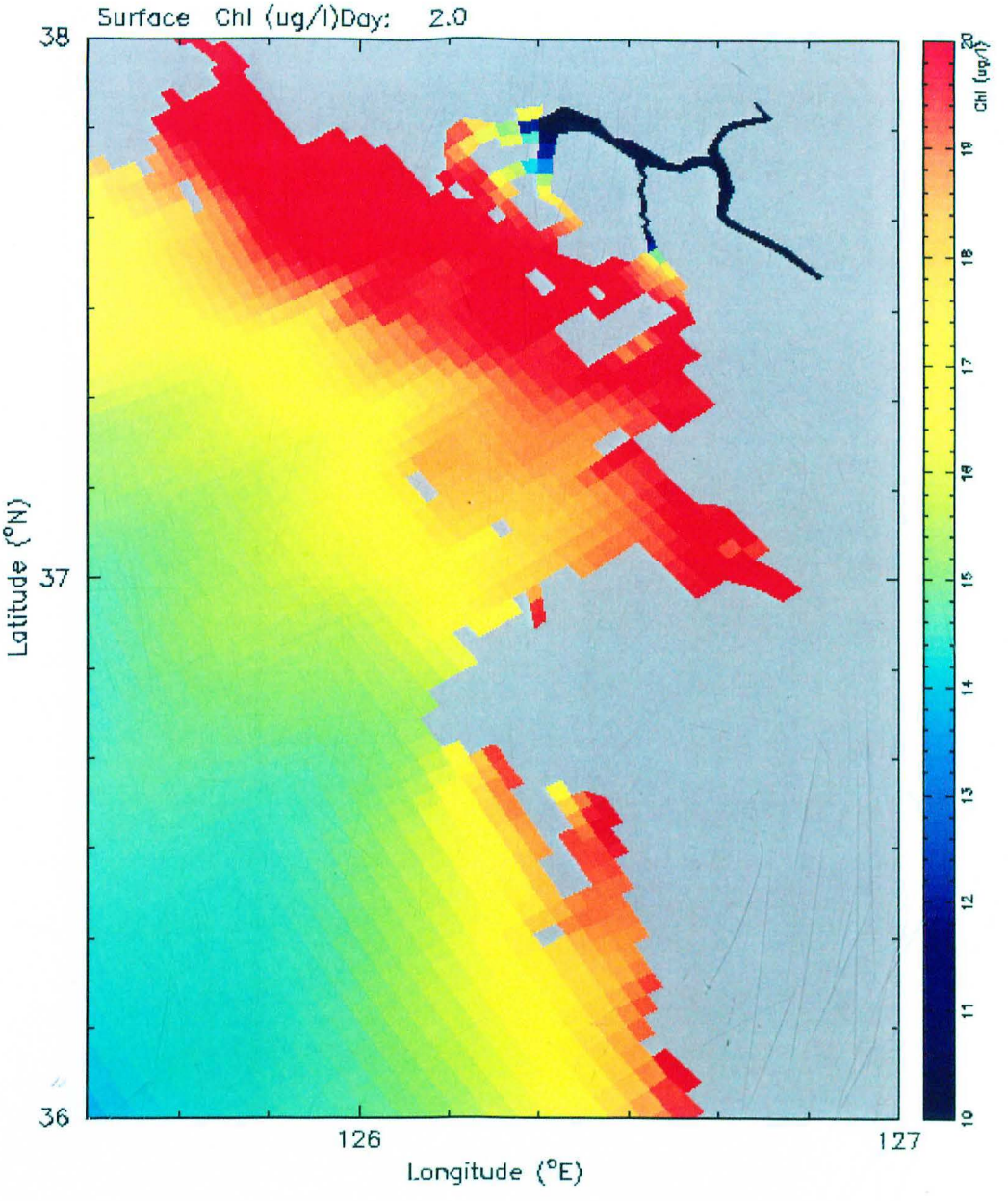

Figure A9. Surface Chlorophyll (μg/l) at day 2

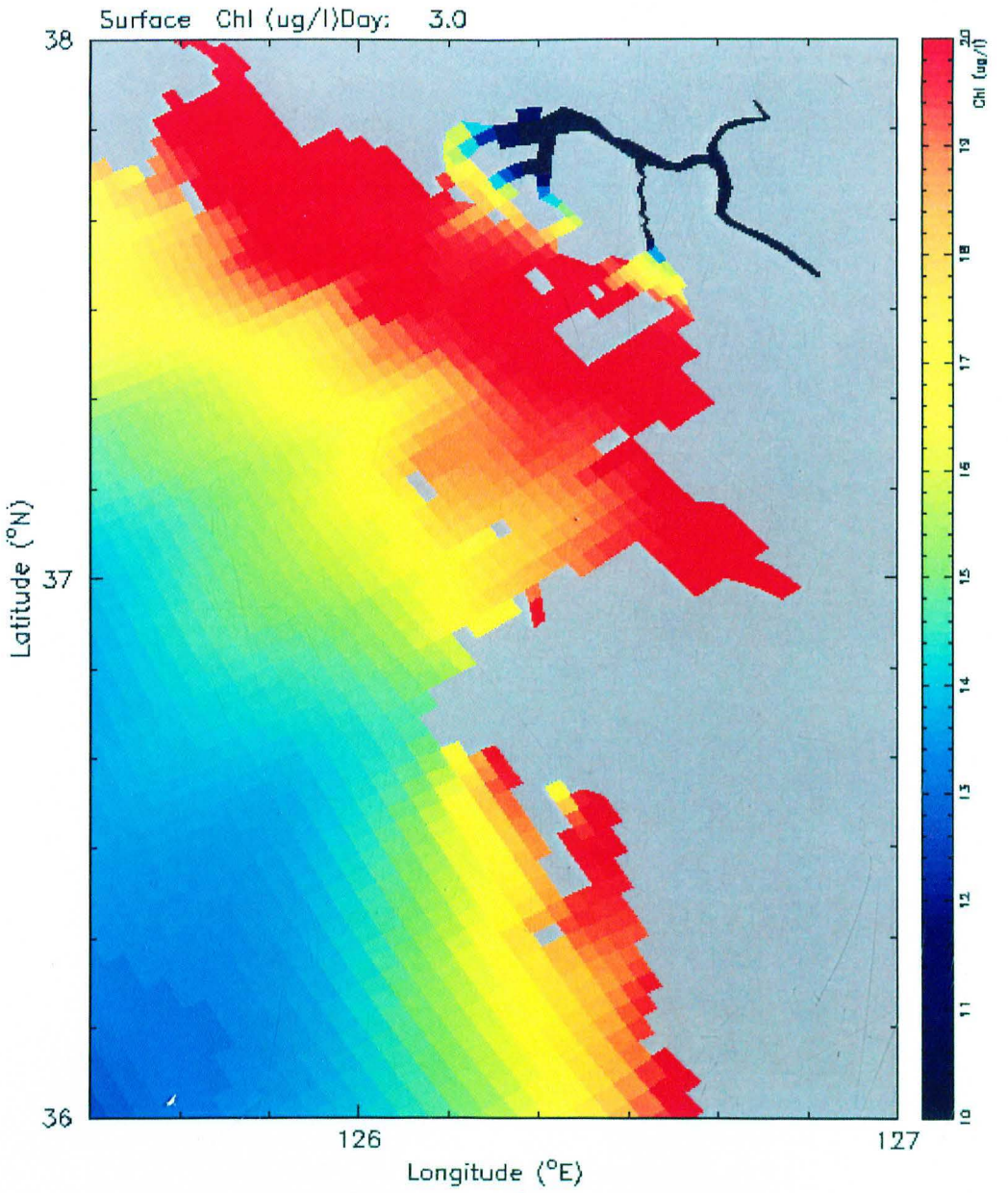

Figure A10. Surface Chlorophyll (μg/l) at day 3

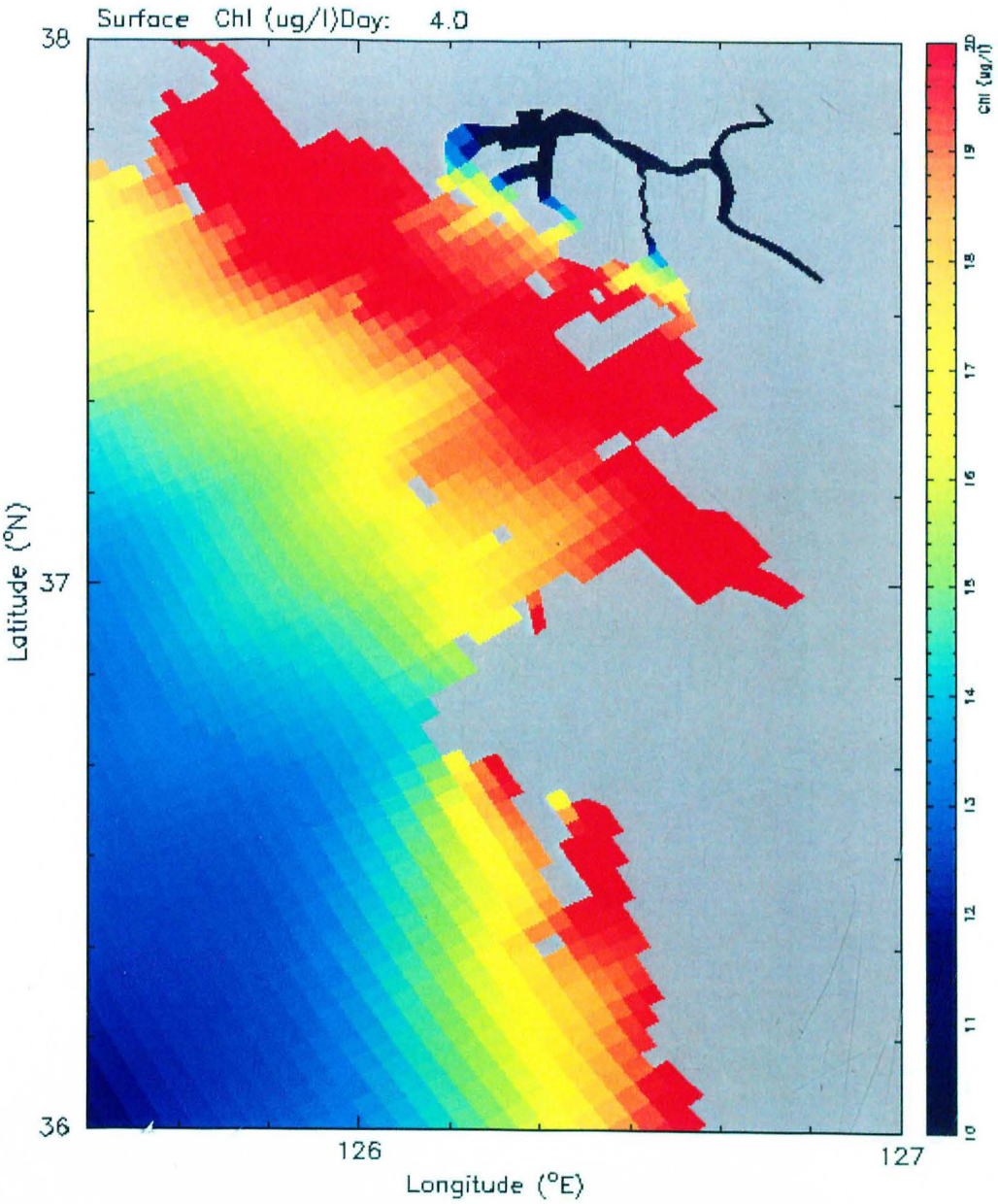

Figure A11. Surface Chlorophyll (µg/l) at day 4

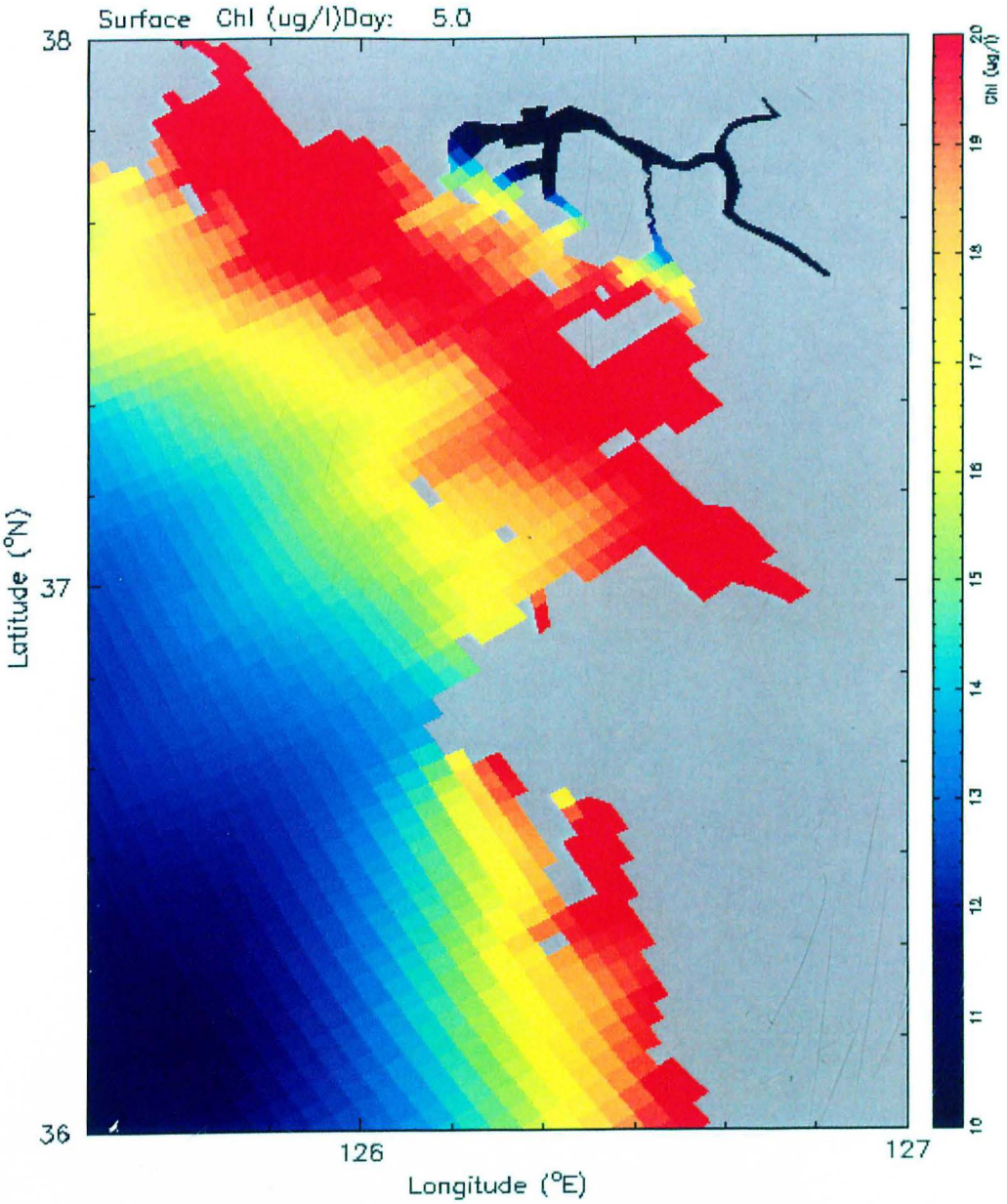

Figure A12. Surface Chlorophyll (μg/l) at day 5

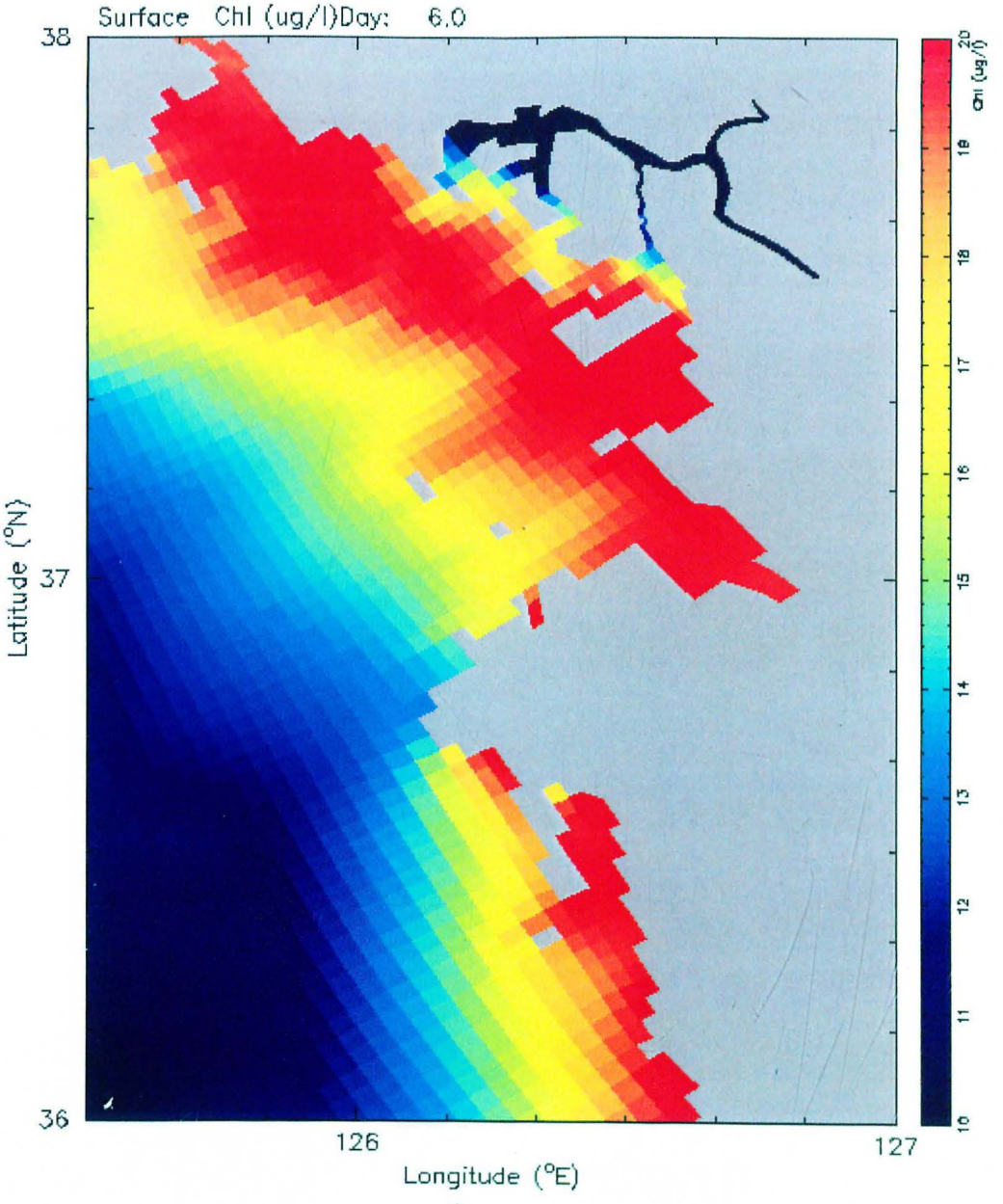

Figure A13. Surface Chlorophyll (μg/l) at day 6

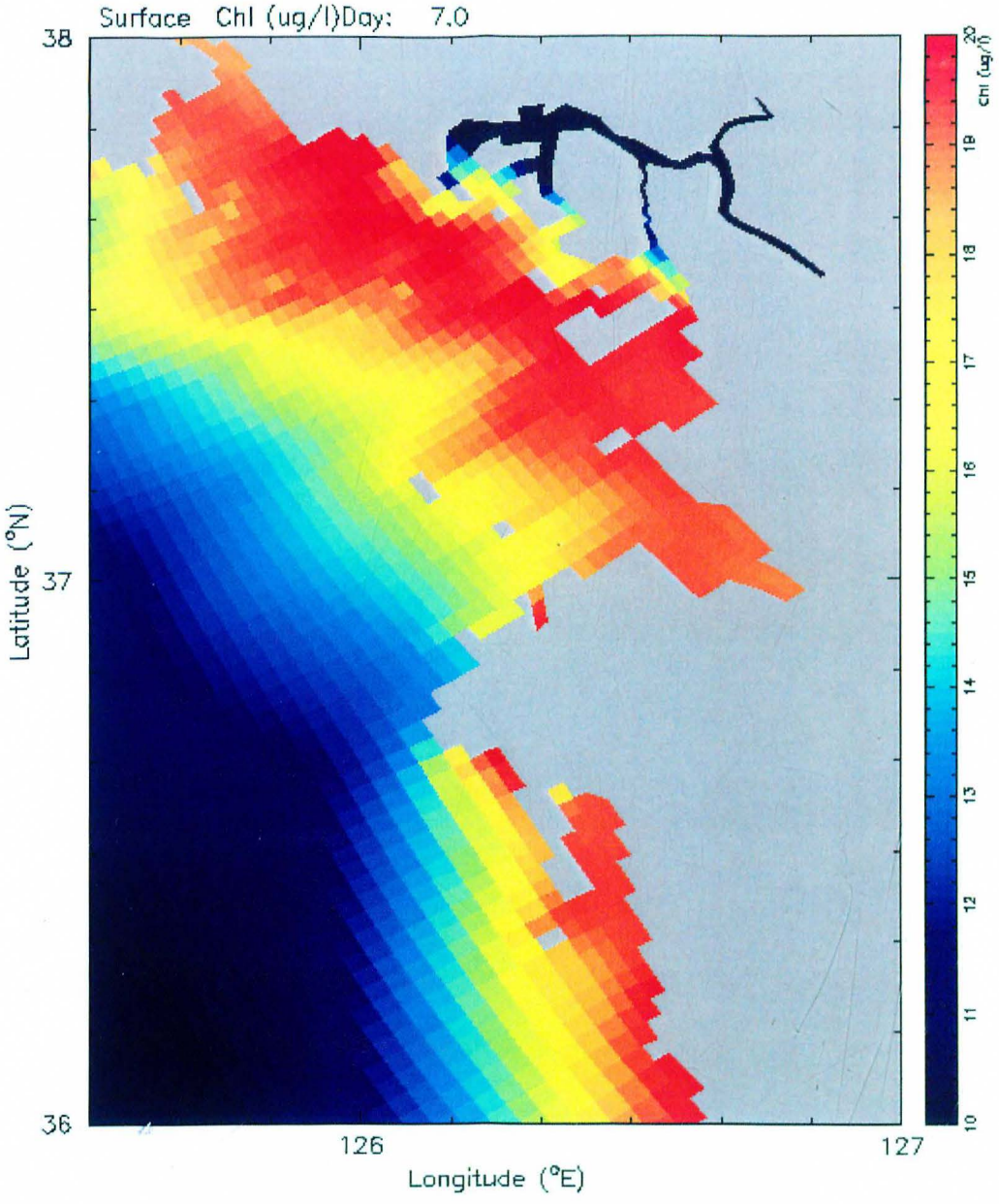

Figure A14. Surface Chlorophyll (µg/l) at day 7

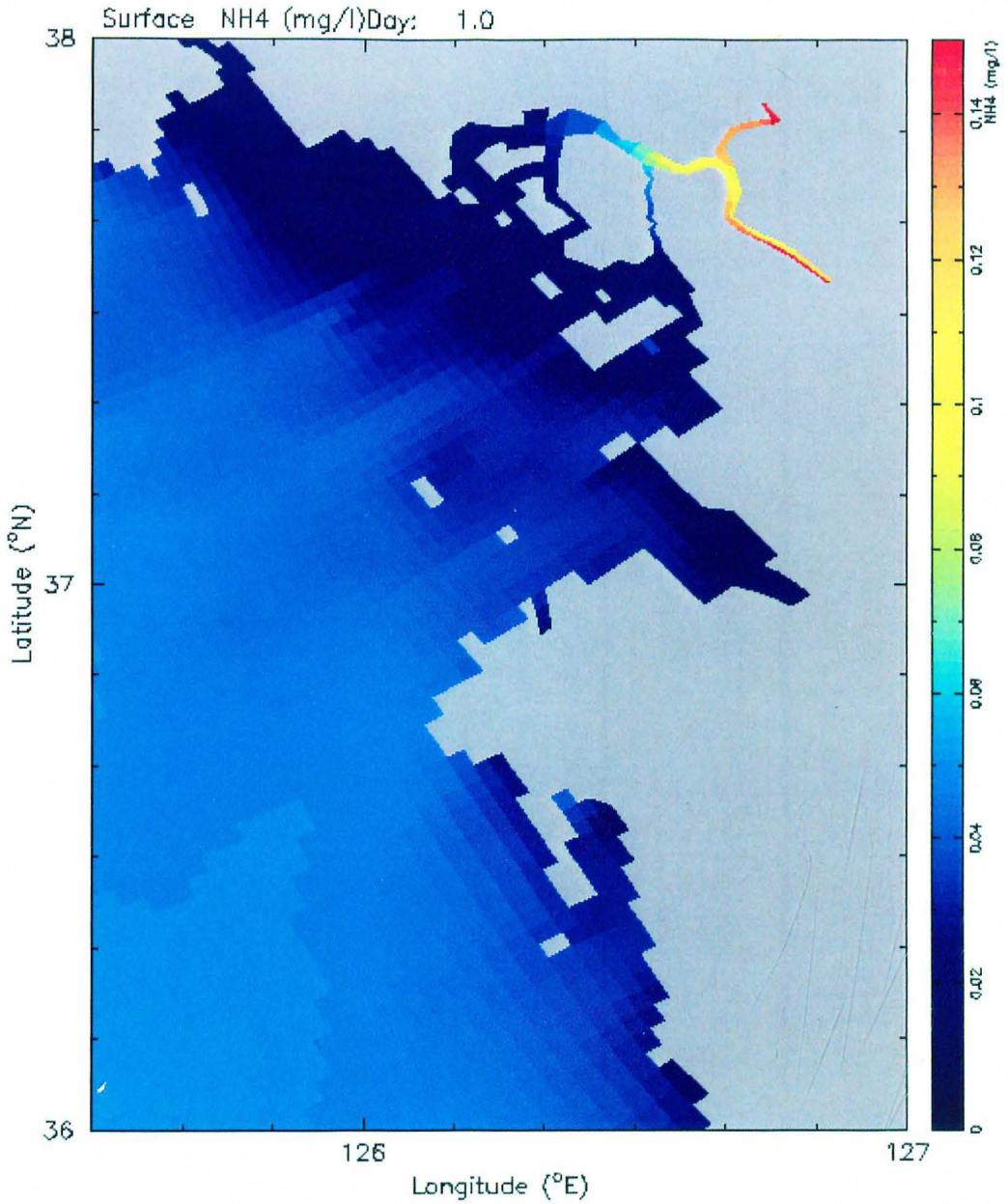

Figure A15. Surface NH_4 (mg/l) at day 1

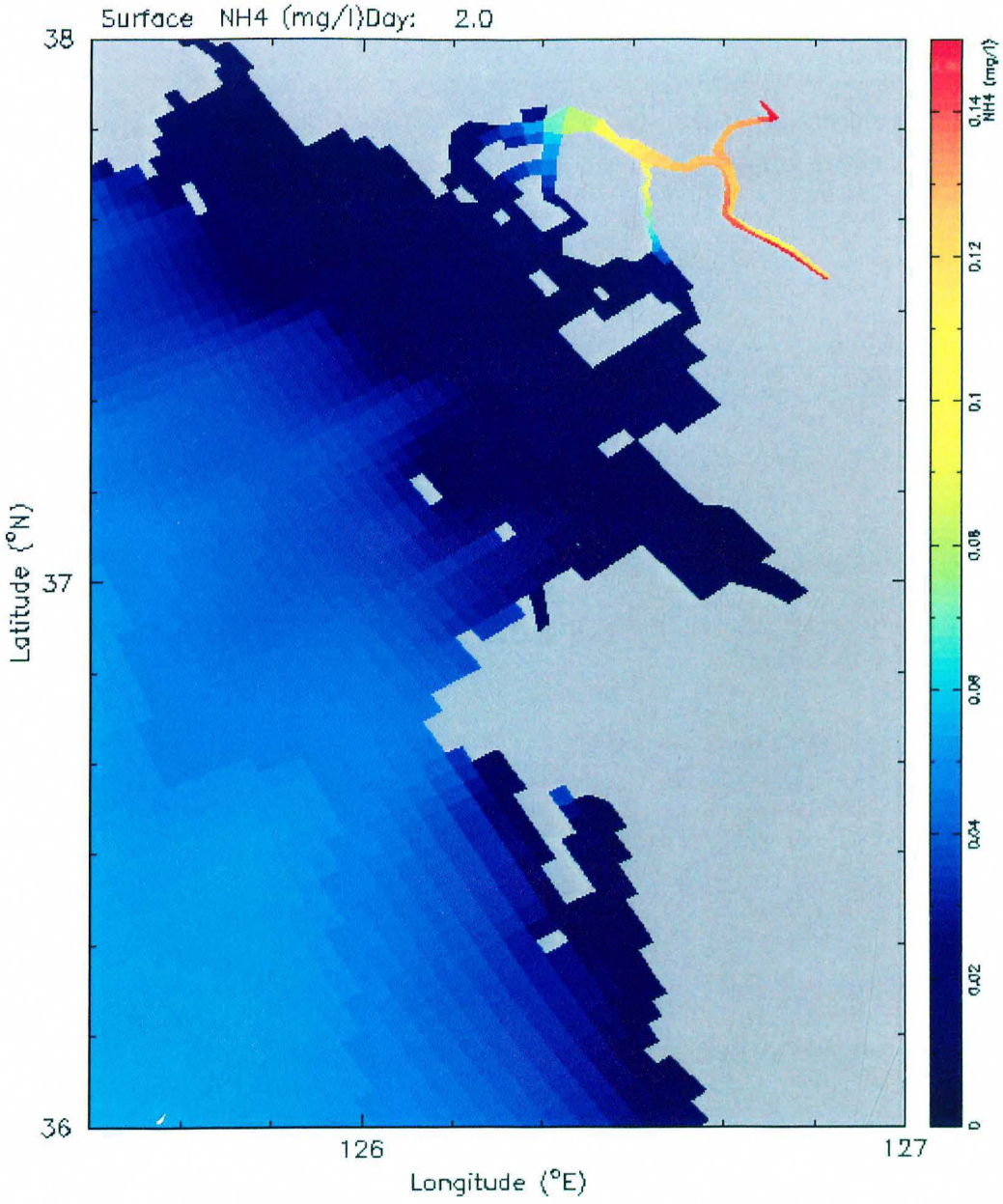

Figure A16. Surface NH_4 (mg/l) at day 2

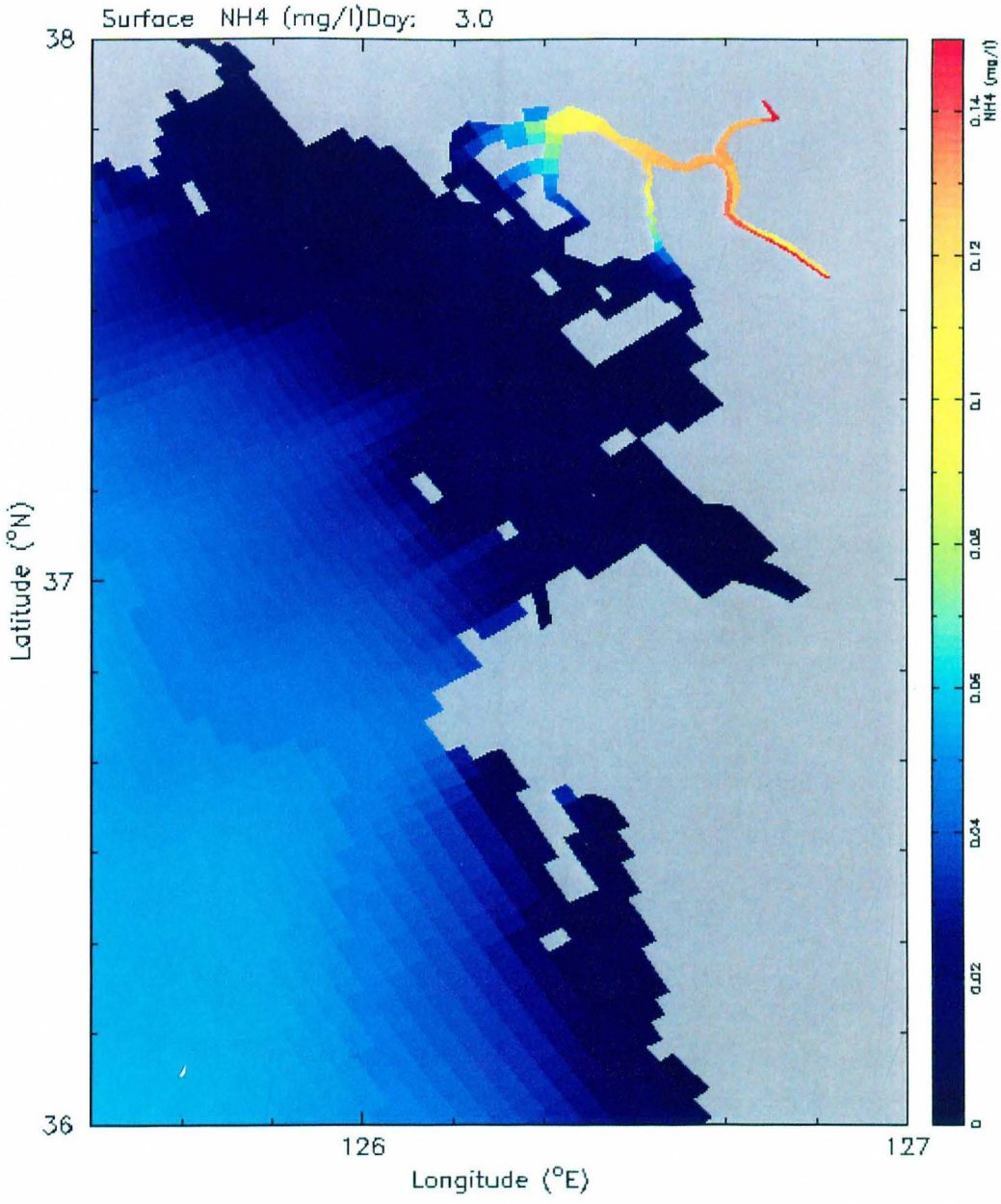

Figure A17. Surface NH_4 (mg/l) at day 3

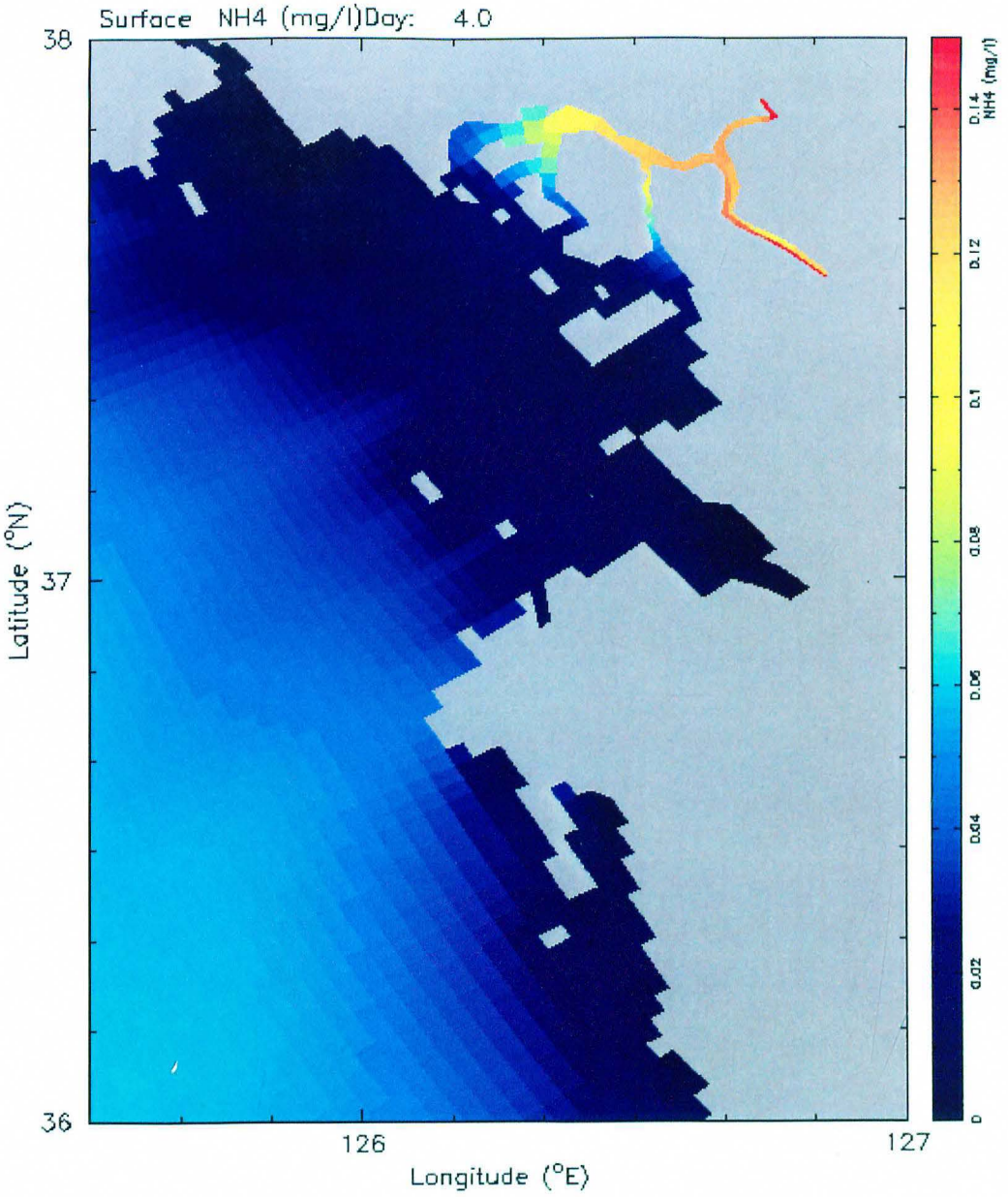

Figure A18. Surface NH_4 (mg/l) at day 4

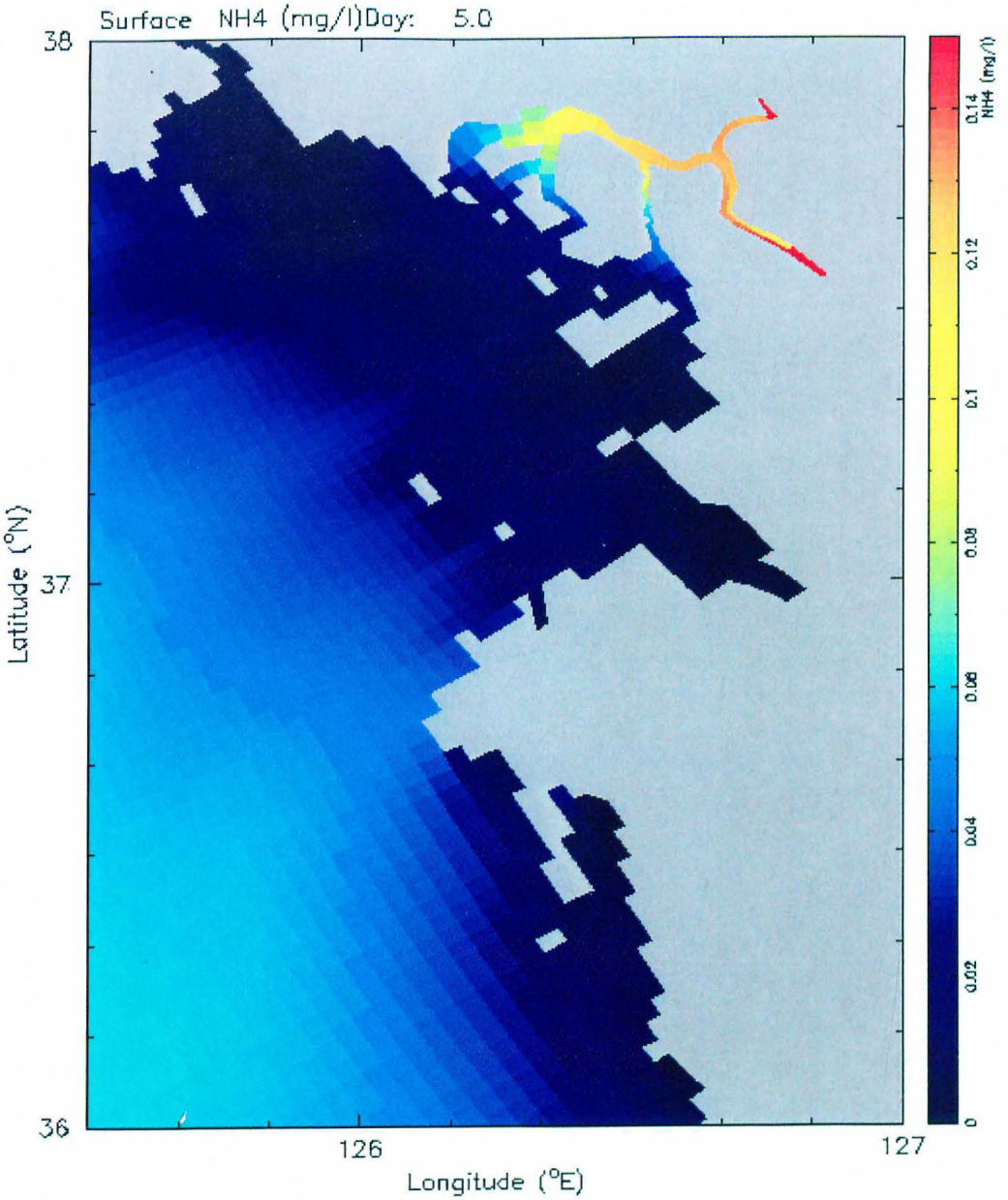

Figure A19. Surface NH_4 (mg/l) at day 5

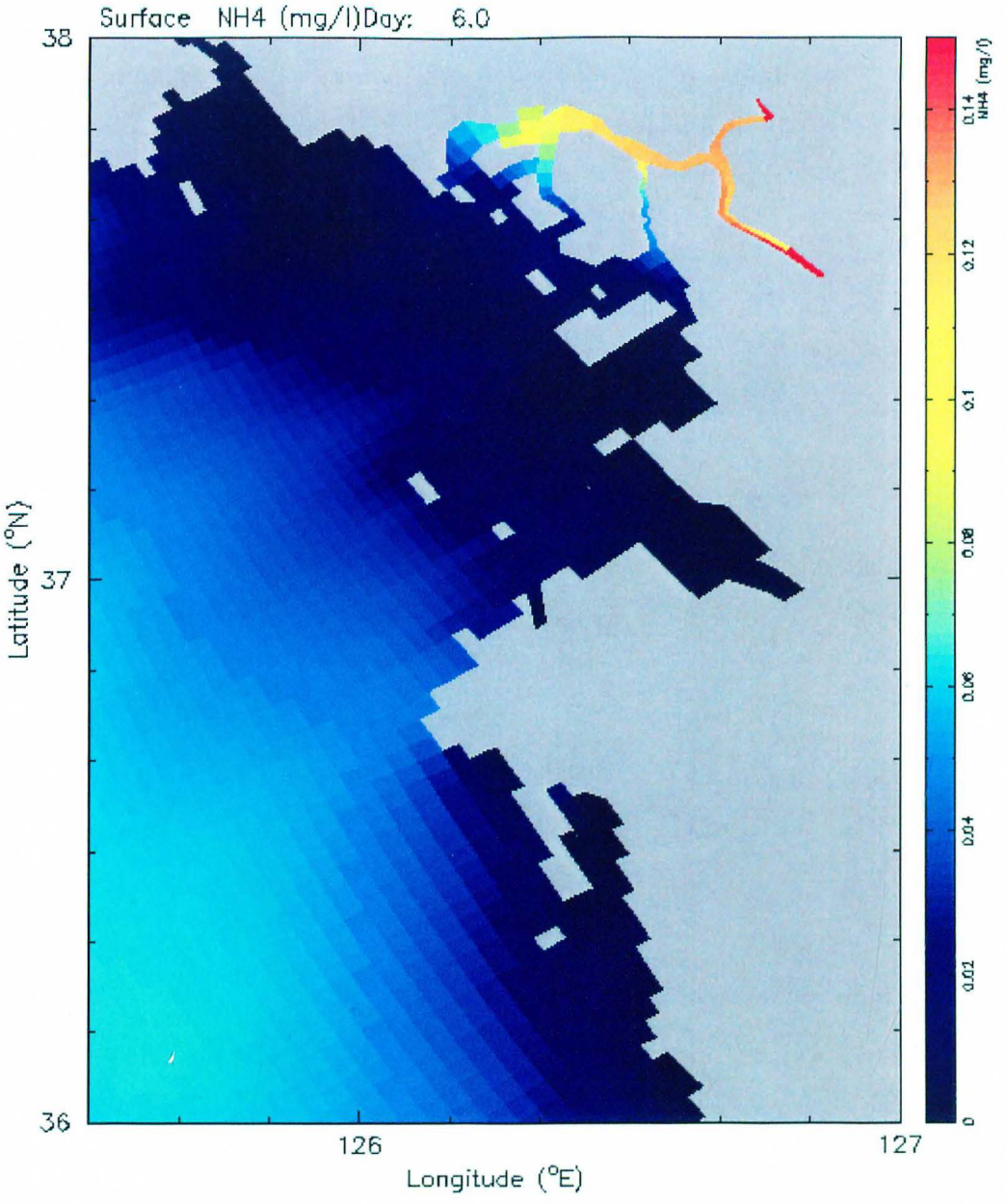

Figure A20. Surface NH_4 (mg/l) at day 6

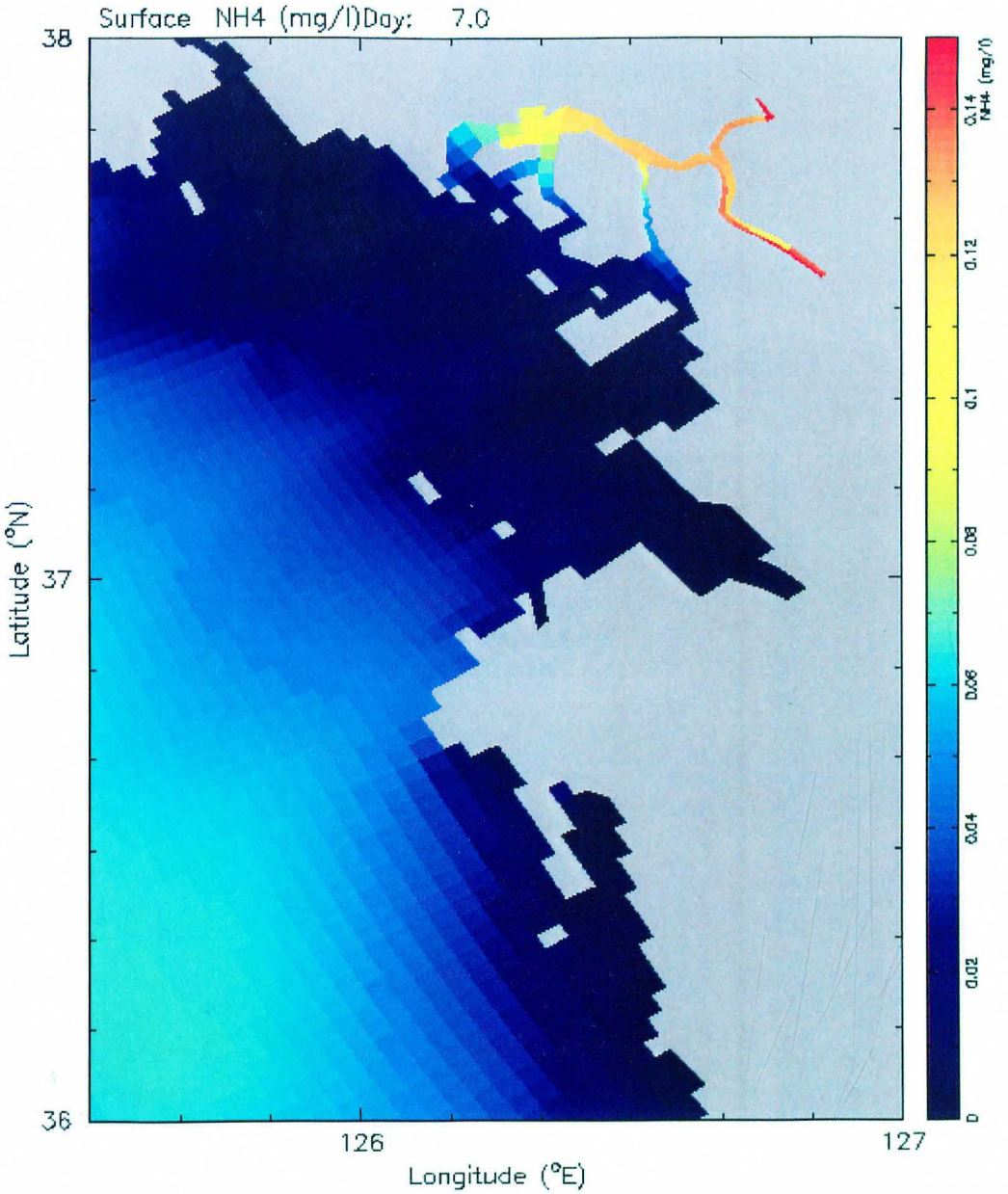

Figure A21. Surface NH_4 (mg/l) at day 7